

2024

Coumarin-Based Aldo-Keto Reductase Family 1C (AKR1C) 2 and 3 Inhibitors

Sravan Jonnalagadda

Ling Duan

Louise F. Dow

Geetha P. Boligala

Elizabeth A. Kosmacek

See next page for additional authors

Tell us how you used this information in this [short survey](#).

Follow this and additional works at: https://digitalcommons.unmc.edu/cop_pharmsci_articles



Part of the [Pharmacy and Pharmaceutical Sciences Commons](#)

Authors

Pravan Jonnalagadda, Ling Duan, Louise F. Dow, Geetha P. Boligala, Elizabeth A. Kosmacek, Kristyn McCoy, Rebecca E. Oberley-Deegan, Yashpal Singh Chhonker, Darryl J. Murry, C. Patrick Reynolds, Barry J. Maurer, Trevor M. Penning, and Paul C. Trippier

Coumarin-Based Aldo-Keto Reductase Family 1C (AKR1C) 2 and 3 Inhibitors

Sravan K. Jonnalagadda,^[a] Ling Duan,^[b] Louise F. Dow,^[a] Geetha P Boligala,^[c] Elizabeth Kosmacek,^[d] Kristyn McCoy,^[c] Rebecca Oberley-Deegan,^[d, e] Yashpal Singh Chhonker,^[f] Darryl J. Murry,^[e, f, g] C. Patrick Reynolds,^[c] Barry J. Maurer,^[c] Trevor M. Penning,^[b] and Paul C. Trippier*^[a, e, g]

A series of 7-substituted coumarin derivatives have been characterized as pan-aldo-keto reductase family 1C (AKR1C) inhibitors. The AKR1C family of enzymes are overexpressed in numerous cancers where they are involved in drug resistance development. 7-hydroxy coumarin ethyl esters and their corresponding amides have high potency for AKR1C3 and AKR1C2 inhibition. Coumarin amide **3a** possessed IC₅₀ values of 50 nM and 90 nM for AKR1C3 and AKR1C2, respectively, and exhibits 'drug-like' metabolic stability and half-life in human and mouse liver microsomes and plasma. Compound **3a** was employed as a chemical tool to determine pan-AKR1C2/3 inhibition effects both as a radiation sensitizer and as a

potentiator of chemotherapy cytotoxicity. In contrast to previously reported pan-AKR1C inhibitors, **3a** demonstrated no radiation sensitization effect in a radiation-resistant prostate cancer cell line model. Pan-AKR1C inhibition also did not potentiate the *in vitro* cytotoxicity of ABT-737, daunorubicin or dexamethasone, in two patient-derived T-cell ALL and pre-B-cell ALL cell lines. In contrast, a highly selective AKR1C3 inhibitor, compound **K90**, enhanced the cytotoxicity of both ABT-737 and daunorubicin in the T-cell ALL cell line model. Thus, the inhibitory profile required to enhance chemotherapeutic cytotoxicity in leukemia may be AKR1C isoform and drug specific.

Introduction

Aldo-Keto Reductases (AKRs) are a superfamily of NAD(P)(H)-linked oxidoreductases that reduce various endogenous carbonyl containing substrates such as sugars, steroids, prostaglandins, and lipids. Many AKRs are overexpressed in a broad range of cancers. The AKRs predominately exist in the cytosol as monomers of ~37 kDa.^[1] Isoform expression is tissue specific. For example, non-small cell lung cancer (NSCLC) predominantly express AKR1C1, AKR1C2, AKR1C3 and AKR1B10, colon cancers mainly express AKR1B10, and breast and prostate cancers predominantly express AKR1C3 isoforms.^[3-4] Owing to the overexpression of AKRs in various cancers, AKR may be a biomarker for tumor prognosis while selective AKR inhibitors offer the potential to be developed as chemotherapeutic agents.

Equally important, the ability of AKRs to metabolize a variety of chemotherapeutic agents has implicated their role in chemotherapeutic drug resistance.^[3] We, and others, have reported that highly selective and potent AKR1C3 inhibitors potentiate chemotherapy in a variety of cancer cell line models, including prostate cancer, breast cancer, and acute myeloid leukemia, among others.^[5] Non-specific, pan-AKR1C inhibitors have also been reported to reverse chemotherapeutic drug resistance. Medroxyprogesterone acetate, a pan-AKR1C inhibitor, enhanced the activity of bezafebrate^[18] and vincristine^[19] against primary patient leukemia cell lines. The pan-AKR1C1, -1C2, and -1C3 inhibitor, NCI-PI, has shown similar activities.^[18] Increased expression of AKR1C3 enhanced resistance to ionizing radiation in models of NSCLC, prostate and esophageal

[a] S. K. Jonnalagadda, L. F. Dow, P. C. Trippier
Department of Pharmaceutical Sciences, College of Pharmacy, University of Nebraska Medical Center, Omaha, Nebraska 68106, United States
E-mail: paul.trippier@unmc.edu

[b] L. Duan, T. M. Penning
Center of Excellence in Environmental Toxicology, Department of Systems Pharmacology and Translational Therapeutics, University of Pennsylvania, Philadelphia, Pennsylvania 19104, United States

[c] G. P. Boligala, K. McCoy, C. P. Reynolds, B. J. Maurer
School of Medicine Cancer Center, Texas Tech University Health Sciences Center, Lubbock, Texas 79430, United States

[d] E. Kosmacek, R. Oberley-Deegan
Department of Biochemistry and Molecular Biology, University of Nebraska Medical Center, Omaha, Nebraska 68106, United States

[e] R. Oberley-Deegan, D. J. Murry, P. C. Trippier
Fred & Pamela Buffett Cancer Center, University of Nebraska Medical Center, Omaha, Nebraska 68106, United States

[f] Y. S. Chhonker, D. J. Murry
Department of Pharmacy Practice and Science, College of Pharmacy, University of Nebraska Medical Center, Omaha, NE 68106, USA.

[g] D. J. Murry, P. C. Trippier
UNMC Center for Drug Design and Innovation, University of Nebraska Medical Center, Omaha, Nebraska 68106, United States

Supporting information for this article is available on the WWW under <https://doi.org/10.1002/cmdc.202400081>

© 2024 The Authors. ChemMedChem published by Wiley-VCH GmbH. This is an open access article under the terms of the Creative Commons Attribution Non-Commercial NoDerivs License, which permits use and distribution in any medium, provided the original work is properly cited, the use is non-commercial and no modifications or adaptations are made.

cancers,^[20] whereas the pan-AKR1C inhibitor, methyl jasmonate, increased radiosensitivity in an *in vitro* model of esophageal squamous cell carcinoma.^[23] Thus, pan-AKR1C inhibitors represent potential novel strategies to both counter clinical chemotherapy and radiation resistance mechanisms and to serve as chemical probes to further credential selective versus pan-AKR1C inhibition.

Coumarins have been extensively investigated as anti-cancer, anti-microbial, and anti-inflammatory agents and exhibit antioxidant and neuroprotective properties.^[24] Drug-resistant cancer cell lines and tumor samples generally overexpress AKR proteins due to the stress response induced via the NRF2-Keap1 pathway.^[3, 28] Coumarin analogs are known to modestly increase NRF-mediated AKR protein expression. AKR1C1, AKR1C2, AKR1C3 were reported to increase 1.6-, 1.4- and 1.3-fold, respectively, when treated with NRF2 activator, 2-hydroximino-

2-phenylethoxy coumarin (Figure 1), in a tongue squamous cell carcinoma cell line containing an antioxidant response element (ARE)-driven luciferase reporter (HSC3-ARE9). An *N*-oxime coumarin increased AKR1C1 expression in HSC-3 cells.^[29] In another study, 7-hydroxy coumarin induced the expression of AKR1C3 in human 1321 N1 astrocytoma cancer cells,^[30] while 7-hydroxyimino coumarin carboxamides (Figure 1) were identified as potent AKR1B10 inhibitors.^[31] HT-29 human colon cancer cells pretreated with this compound showed increased sensitivity to mitomycin-C.^[33] *Peucedanum japonicum* flower extracts that contain coumarins inhibited AKR1C1 activity when tested in the A549 human NSCLC cell line.^[34] Recently, Endo *et al.* reported a series of 8-hydroxy-2-imino-*N*-(*p*-substituted)-2*H*-chromene-3-carboxamides as potent and selective AKR1C3 inhibitors with IC₅₀'s of 25–56 nM and >220-fold selectivity compared to AKR1C1 and AKR1C2. These compounds inhibited

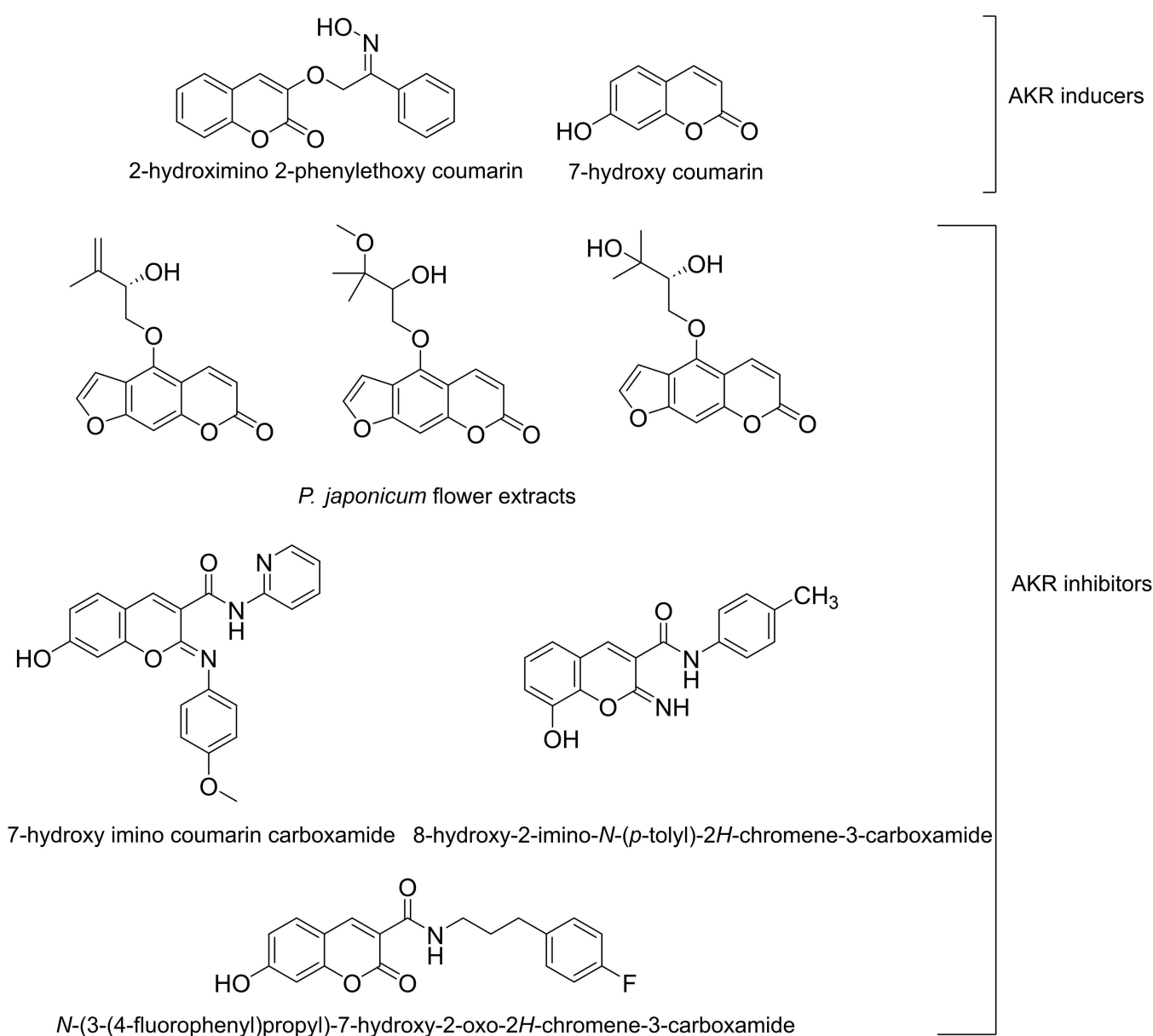


Figure 1. Structures of known coumarin-based AKR inducers/inhibitors.

cell proliferation in human prostate cancer cell lines, *in vitro* and suppressed tumor growth in a human prostate cancer mouse xenograft model.^[12] Here, we report the synthesis of highly potent, nanomolar coumarin-based inhibitors of AKR1C2 and AKR1C3 and demonstrate that they provide no radio-sensitization effects in 22Rv1 human prostate cancer cells nor potentiate drug effects in human leukemia cell lines, compared to a highly selective AKR1C3 inhibitor.

Results and Discussion

Chemistry

We first synthesized various substituted coumarin carboxylic acid ethyl esters **1a–1g** via Knoevenagel condensation of substituted salicylaldehydes with diethyl malonate in the presence of piperidine (Scheme 1). Ethyl esters **1c** and **1g** were further hydrolyzed using sodium hydroxide in ethanol-water to obtain 7-methoxy and 7-*N,N*-diethyl coumarin carboxylic acids **1h** and **1i**. To probe the importance of the 7-hydroxy position, we also synthesized 7-amino coumarin carboxylic acid ethyl ester **1j**, derived from 7-bromo coumarin carboxylic acid ethyl ester **1e** through treatment with sodium azide and subsequent Pd/C-mediated reduction.

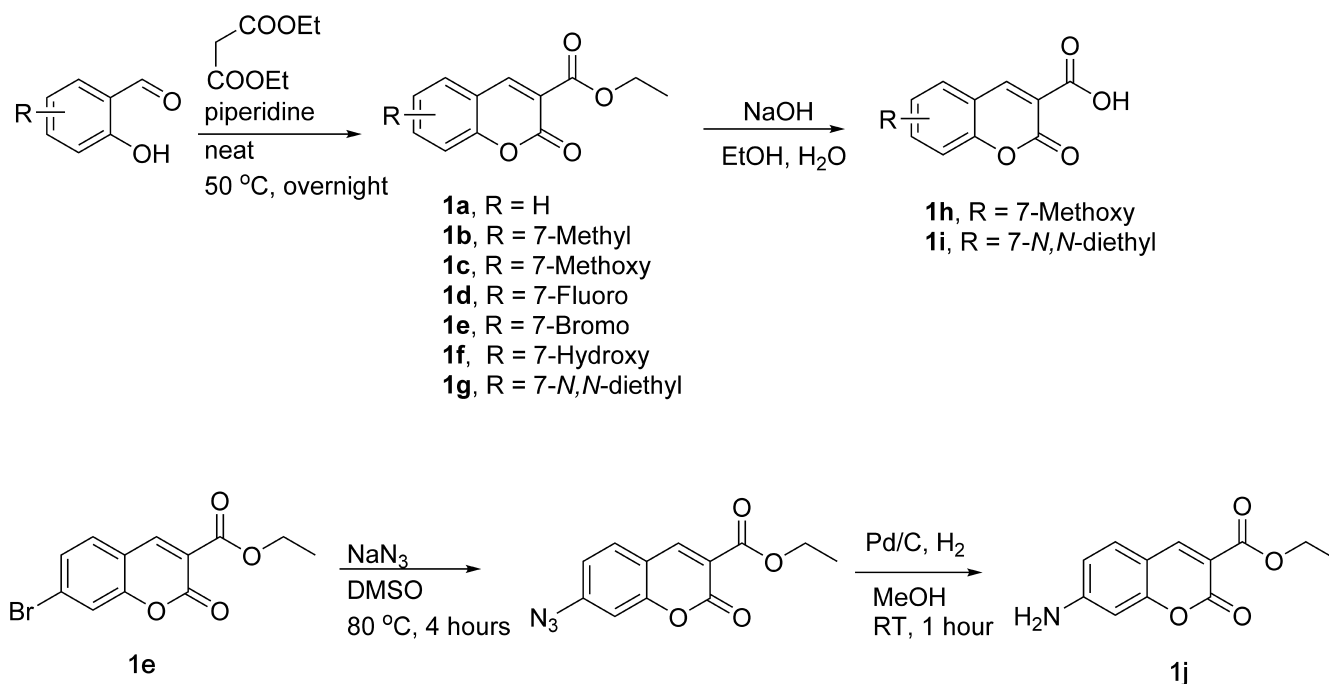
Ethyl ester **1f** was hydrolyzed with NaOH to obtain carboxylic acid **1k**, followed by acetylation with acetic anhydride to afford **1l**. Acetyl coumarin acid **1l** was then subjected to amide bond formation with the corresponding benzyl amine in the presence of EDC, HOBT and DIPEA. The resulting 7-acetyl coumarin benzyl amides were then reacted with NaOH to obtain 7-hydroxy coumarin amides **2a–2e** (Scheme 2). Addi-

tionally, the reaction with 2-phenylethyl amine was undertaken to obtain **2f** to observe the effect of one carbon homologation.

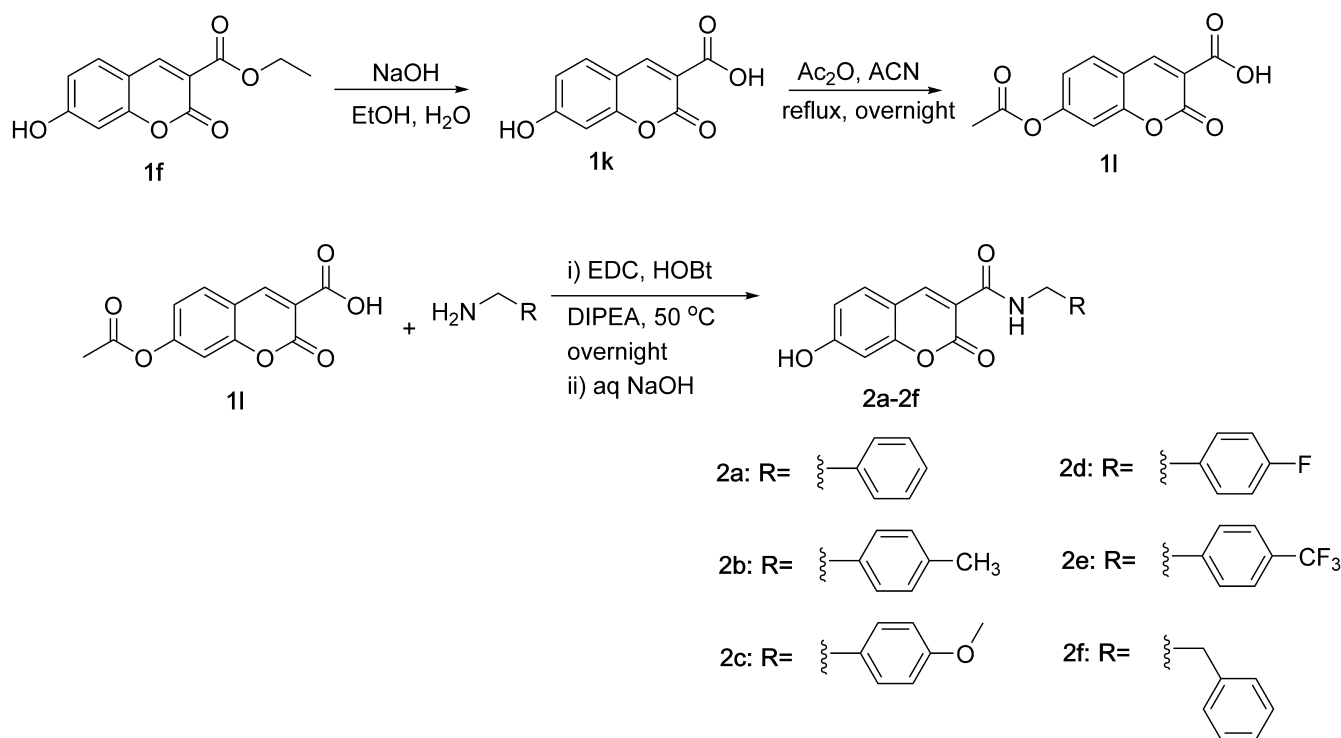
In addition to benzyl amines, we also explored the aliphatic amines: *N,N*-diethyl amine (**3a**), piperidine (**3b**) and *N,N*-diethylpyrrolidine-2-carboxamide (**3c**), which were obtained as depicted (Scheme 3). We also synthesized simple coumarin phenyl amides **3d** and **3e** to explore the requirement of the methylene group to AKR1C inhibition (Scheme 3).

Previously, we identified several prenyl containing cinnamic acids that showed potent and selective AKR1C3 inhibition.^[5] To determine whether selective AKR1C3 inhibitory activity is retained, we synthesized coumarin derivatives with *O*-prenyl and cinnamic acid substitutions at the 7- and 6-positions, respectively (Scheme 4). The 7-hydroxy group of **1f** was prenylated using a mild base to obtain *O*-prenyl coumarin carboxylic acid ethyl ester **4a**. Upon hydrolysis, *O*-prenyl coumarin carboxylic acid **4b** was obtained. Cinnamic acid derivative **4c** was prepared from Heck coupling of 6-bromo coumarin carboxylic acid ethyl ester and *tert*-butyl acrylate in the presence of catalytic Pd(OAc)₂ and P(*p*-OCH₃Ph)₃. Silica gel treatment resulting in the hydrolysis of the *tert*-butyl group to form cinnamic acid coumarin carboxylic acid ethyl ester **4c**.

Phenyl sulfonyl coumarin derivative **5** was obtained by alkylation of thiophenol with ethyl 2-bromoacetate in the presence of K₂CO₃ to obtain ethyl 2-(phenylthio)acetate, which was oxidized using oxone to afford ethyl 2-(phenylsulfonyl)acetate. 2,4-dihydroxybenzaldehyde and ethyl 2-(phenylsulfonyl)acetate were condensed in the presence of piperidine to provide phenyl sulfonyl coumarin **5** (Scheme 5).



Scheme 1. Synthesis of substituted coumarin carboxylic acid derivatives **1a–j**.



Scheme 2. Synthesis of 7-hydroxy coumarin benzyl amides 2a–2f.

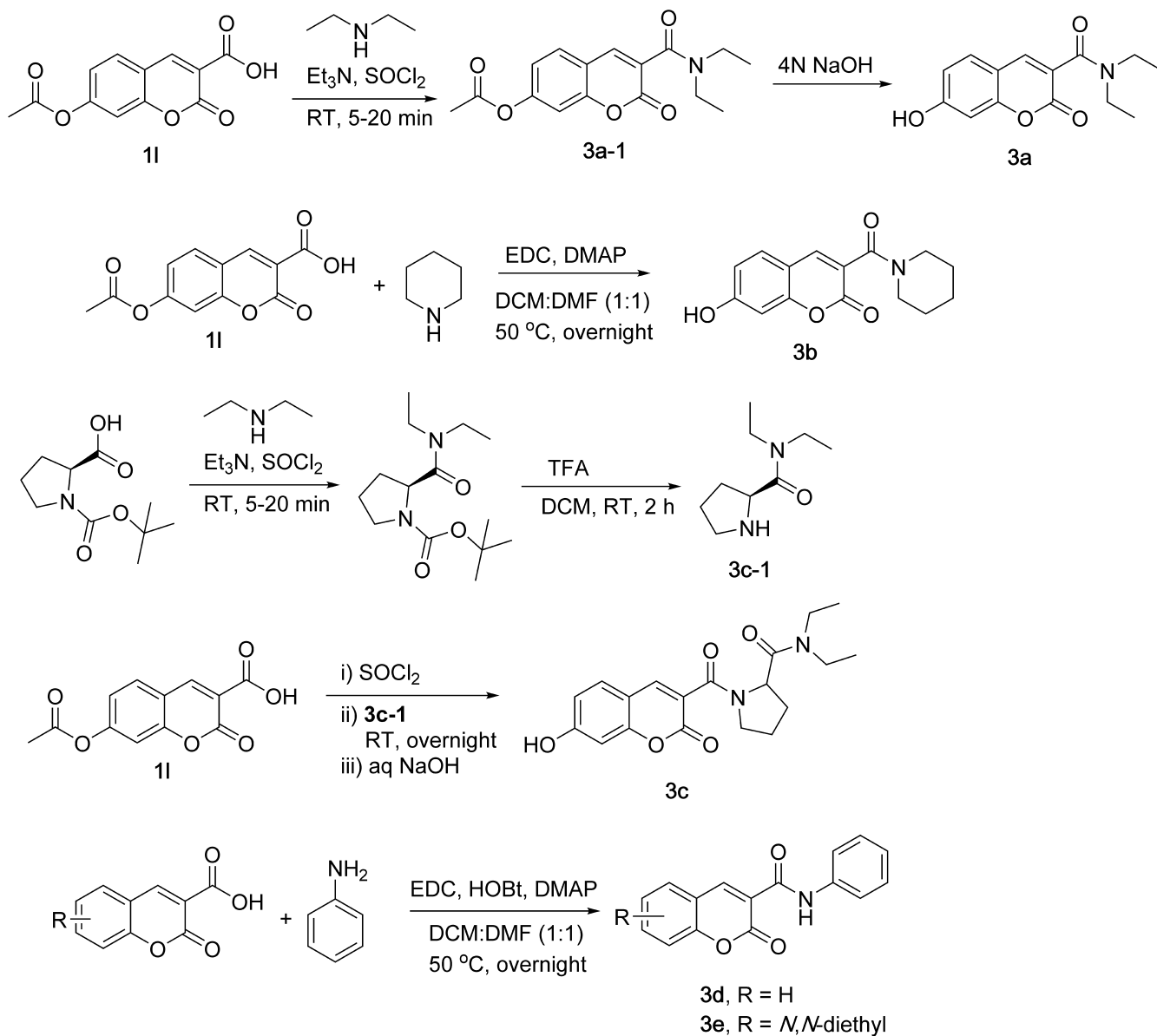
Structure-Activity Relationship

The synthesized coumarin carboxylic acid ethyl esters **1a–1g** were tested for AKR1C3 inhibition by measuring the NADP⁺ dependent oxidation of *S*-tetralol catalyzed by the enzyme as previously reported (Table 1).^[5] The most active compounds were selected for further inhibition studies against AKR1C1, AKR1C2 and AKR1C4. Unsubstituted coumarin ethyl ester **1a** possessed an IC₅₀ of 6.4 μM versus AKR1C3. Methyl substitution at the 7-position (**1b**) increased potency with an IC₅₀ of 2.3 μM while 7-methoxy substitution (**1c**) significantly enhanced potency with an IC₅₀ of 180 nM. Screening of electron-withdrawing substituents at this position, using 7-bromo (**1e**) and 7-fluoro (**1d**), reduced potency and yielded IC₅₀ values of 2.6 and 7.8 μM respectively, where decreased potency was seen with an increased electron-withdrawing effect. Further exploration of electron-donating groups afforded 7-hydroxy analogue **1f** which gave an IC₅₀ of 93 nM and the *N,N*-diethyl derivative **1g** gave an IC₅₀ of 480 nM. Thus, suggesting a hydrogen bond acceptor at this position of the coumarin scaffold is essential for potency, an observation further supported by the activity of amine **1j** (IC₅₀ of 105 nM).

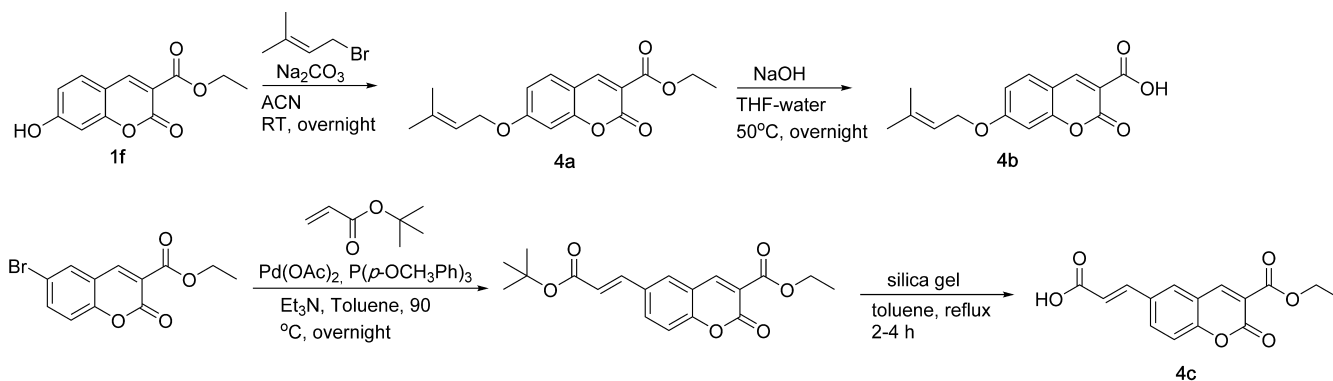
To evaluate whether the ethyl ester is required for AKR1C3 inhibition, 7-methoxy and 7-*N,N*-diethyl coumarin carboxylic acids **1h** and **1i** were tested, which showed AKR1C3 IC₅₀ values of 1.22 and 2.73 μM, respectively, compared to IC₅₀ values of 180 and 480 nM for their corresponding ethyl esters **1c** and **1g**, indicating that the ethyl ester enhances activity. Given the use of an isolated enzyme assay, the potential for the carboxylic acid to impair cell penetration is not a relevant consideration.

Based on these results the most potent compound **1f** (IC₅₀ of 93 nM) was evaluated for its inhibitory activity against the other highly homogeneous AKR isoforms 1C1, 1C2 and 1C4, which gave IC₅₀ values of 67, 100 and 606 nM, respectively. Thus, the compound is a pan inhibitor of AKR1C1, AKR1C2 and AKR1C3 with approximately six-fold selectivity over AKR1C4 (Table 1).

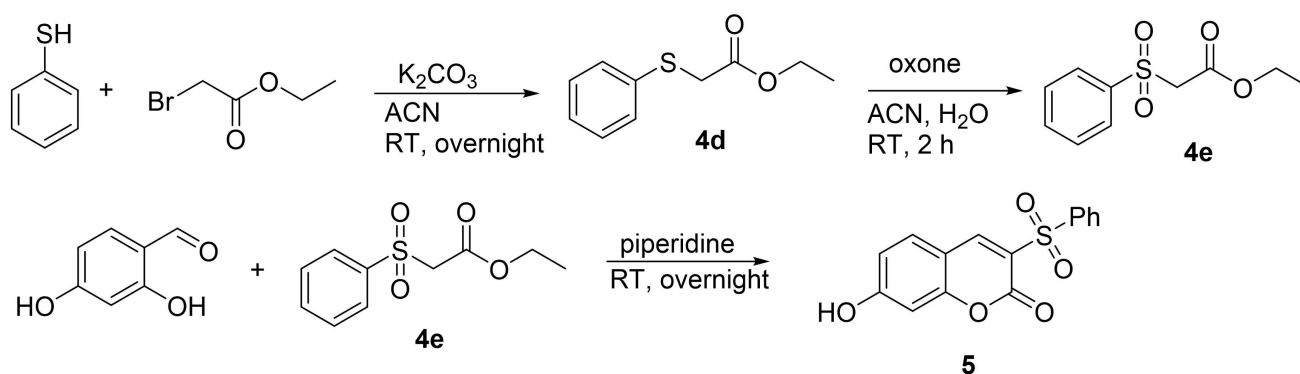
Having identified the 7-hydroxy substituent as a requirement for inhibition potency on the Western fragment of the coumarin scaffold we next turned our attention to the Eastern fragment and a series of benzyl amides. The benzyl amide functionalized coumarins generally possessed excellent AKR1C3 inhibition activity (Table 2). Unsubstituted benzyl amide (**2a**) possessed an IC₅₀ of 160 nM. A substituent scan of the terminal phenyl moiety revealed that both 4-fluoro benzyl amide **2d** and 2-phenyl ethyl amide **2f** gave IC₅₀ values of 60 nM, with 4-methyl benzyl amide **2b** being almost equipotent yielding an IC₅₀ value of 70 nM. Addition of a 4-methoxy substituent (**2c**) afforded an IC₅₀ of 170 nM which was equipotent with the unsubstituted parent compound. Similarly, 4-trifluoromethyl benzyl amide (**2e**) possessed an IC₅₀ of 90 nM, revealing no difference between electronic effects of the substituent. These results show that one carbon homologation does not affect AKR1C3 inhibition, suggesting these compounds occupy an area of the enzyme with a deep pocket. Indeed, coumarin phenyl amide **3d**, with no substitution at the 7-position, resulted in attenuation of AKR1C3 inhibition (IC₅₀ = 47.8 μM). Substitution of the 7-hydroxy moiety with a *N,N*-diethyl group on coumarin benzyl amide **3e** (an analogue of **1i**) also resulted in attenuation of AKR1C3 activity (IC₅₀ = 19.1 μM). *O*-Prenyl coumarin carboxylic acid ethyl ester **4a** possessed AKR1C3 IC₅₀



Scheme 3. Synthesis of 7-hydroxy coumarin aliphatic amides 3a–3e.



Scheme 4. Synthesis of prenyl coumarin (4a–b) and cinnamic acid coumarin (4c) derivatives.



Scheme 5. Synthesis of phenyl sulfonyl coumarin derivative.

of 5.37 μM , whereas the hydrolyzed product **4b** exhibited an improved AKR1C3 IC_{50} of 1.09 μM . Cinnamic acid coumarin ester **4c** showed attenuated activity with an IC_{50} of 2.78 μM .

Amides **3a–3c** exhibited slightly more potent AKR1C3 inhibition compared to substituted benzyl amides (Table 2). *N,N*-diethyl amide **3a** and piperidine amide **3b** both possessed an AKR1C3 IC_{50} of 50 nM, while proline *N,N*-diethyl amide **3c** possessed an AKR1C3 IC_{50} of 40 nM. Protection of the 7-hydroxy group in **3a** as its acetate eliminated the inhibitory potency of the compound. Overall, these data clearly indicate the importance of the 7-hydroxy group and the methylene spacer within the amide group but illustrate no requirement for an aromatic ring.

Based on their potent AKR1C3 inhibitory effects, we evaluated compounds **1j**, **2b**, **2d**, **2e**, **2f**, **3a–3c**, **4a** and **4b** for AKR1C2 inhibition. Interestingly, most of the analogues showed similar AKR1C2 inhibition with no selectivity towards AKR1C3 inhibition (Table 2). Compounds **1j**, **2b**, **2d**, **2e**, **2f**, **4b** and **5** all showed equipotent pan-activity within experimental error. *N,N*-diethyl amide **3a** and piperidine amide **3b** both possessed AKR1C2 IC_{50} of 90 nM whereas proline *N,N*-diethyl amide **3c** showed an AKR1C2 IC_{50} of 100 nM which provides a slight 2:1 preference for inhibition of AKR1C3. These results indicate that 7-hydroxy coumarin amides show potent AKR inhibition with no selectivity towards either AKR1C3 or AKR1C2 and these derivatives could be employed as pan-AKR1C inhibitors.

To explain the promiscuous nature of AKR1C3 and AKR1C2 inhibition by compound **3a**, we employed *in silico* docking (Figure 2). The crystal structure of the AKR1C3 ternary complex with NADP^+ and the AKR1C3 selective chromene derivative **2j** (PDB ID: 7C7G),^[12] was imported into SeeSAR (12.1, BioSolveIT, GmbH, Sankt Augustin, Germany) and prepared for docking. The **2j** ligand was removed and a 26 amino acid residue binding site was defined. Docking simulations afforded binding poses scored by HYDE as previously described.^[35]

Hydrogen bond formation between the 7-OH of **3a** and HIS-117 in the crucial oxyanion site was predicted, but not with TYR-55, along with formation of a hydrogen bond between the lactone carbonyl and Ser-118, which is unique to AKR1C3 (Figure 2A), rationalizing the observed potency to inhibition of AKR1C3. The crystal structure of AKR1C2 (PDB ID: 4JQ4) was

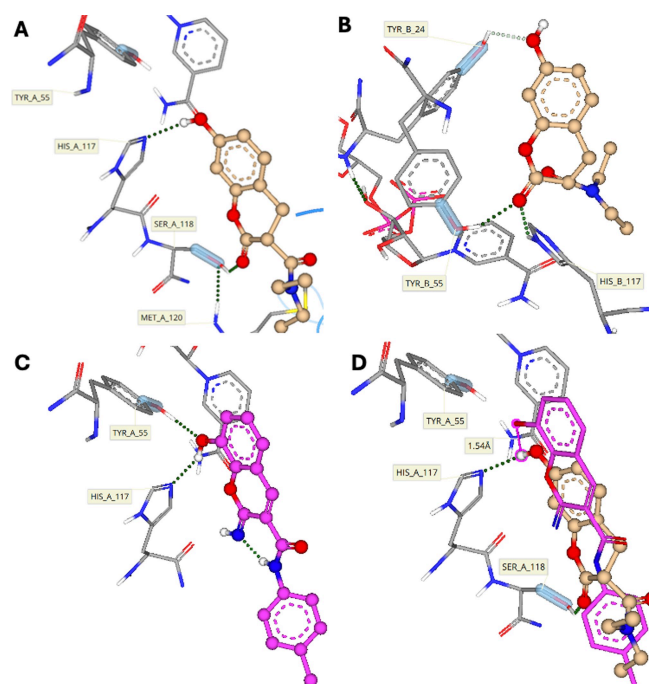


Figure 2. Docking pose and predicted hydrogen bond interactions (green dotted lines) of compounds **3a** (Gold) and chromene-based AKR1C3 inhibitor **2j** (magenta). A) **3a** docked into the crystal structure of AKR1C3. B) **3a** docked into the crystal structure of AKR1C2. C) **2j** docked into the crystal structure of AKR1C3. D) Overlay of **3a** and **2j** within AKR1C3.

then used for docking with a 25 amino acid residue binding site defined. The 7-OH moiety of **3a** was predicted to form a hydrogen bond to the TYR-24 residue of AKR1C2, while the lactone carbonyl was predicted to form a hydrogen bond with TYR-55 and HIS-117 (Figure 2B). Thus, the 7-OH of **3a** prevents binding of TYR-55 of AKR1C3 while allowing binding to TYR-24 of AKR1C2, rationalizing the potency of **3a** for AKR1C2 inhibition. The 8-OH of the chromene ligand **2j** is positioned to form hydrogen bonds with both HIS-117 and TYR-55 of AKR1C3 (Figure 2C), as confirmed by co-crystal structure.^[12] Overlay of **2j** (magenta) and **3a** (gold) illustrates the relative positioning of the OH moiety in the oxyanion site of AKR1C3. The 7-OH of **3a** is remote from TYR-55 prohibiting hydrogen bond formation while the 8-OH of **2j** is well positioned to form hydrogen bonds

Table 1. Activity of compounds 1 a–1 j to inhibit AKR1C1, C2, C3 and C4 family members.

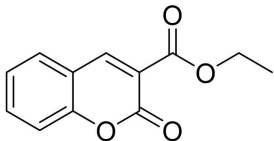
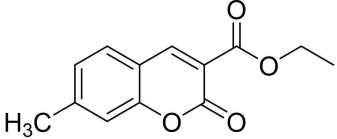
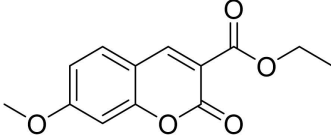
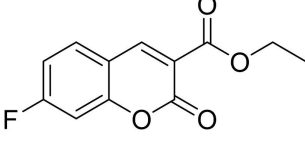
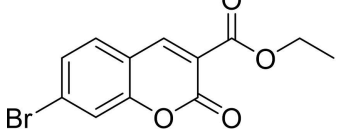
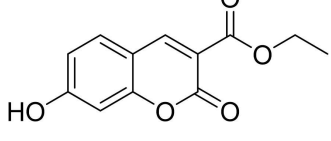
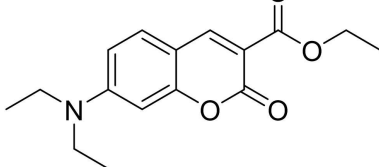
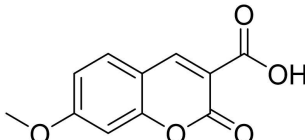
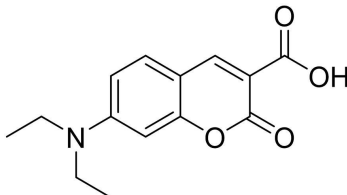
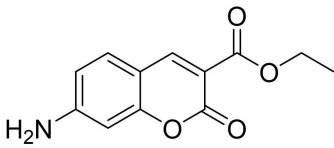
No.	Compound	AKR1C3 IC ₅₀ * (μM)	AKR1C1 IC ₅₀ * (μM)	AKR1C2 IC ₅₀ * (μM)	AKR1C4 IC ₅₀ * (μM)
1a		6.40 ± 0.71	ND ^[a]	ND	ND
1b		2.33 ± 0.40	ND	ND	ND
1c		0.180 ± 0.037	ND	ND	ND
1d		7.83 ± 0.95	ND	ND	ND
1e		2.59 ± 0.36	ND	ND	ND
1f		0.093 ± 0.008	0.0673 ± 0.0045	0.10 ± 0.01	0.6058 ± 0.0743
1g		0.48 ± 0.04	ND	ND	ND
1h		1.22 ± 0.17	ND	0.67 ± 0.07	ND
1i		2.73 ± 0.11	ND	3.40 ± 0.17	ND

Table 1. continued					
No.	Compound	AKR1C3 IC ₅₀ * (μM)	AKR1C1 IC ₅₀ * (μM)	AKR1C2 IC ₅₀ * (μM)	AKR1C4 IC ₅₀ * (μM)
1j		0.105 ± 0.035	ND	0.169 ± 0.064	ND
*Values represent the mean ± SEM of n = 3 experiments. ^(a) ND = not determined.					

to both HIS-177 and TYR-55, with a predicted distance of 1.54 Å between the 7-OH and 8-OH moieties (Figure 2D).

Microsomal Metabolic and Mouse Plasma Stability

Owing to the potency of *N,N*-diethyl amide **3a** for pan-AKR1C inhibition and the requirement of the amide bond connecting to a benzyl or aliphatic moiety as pharmacophoric, we tested this analogue to determine its *in vitro* pharmacokinetic profile in mouse liver microsomes (MLM) and human liver microsomes (HLM) (Figure 3A). Compound **3a** was found to be stable in both negative control microsomal incubations (without NADPH) and in mouse and human liver microsomes with NADPH, for 60 minutes. Indicating stability of the essential amide bond. Compound **3a** was stable in mouse plasma up to four hours with > 90% of the parent remaining at the final collection time point (Figure 3B).

Inhibition of Prostate Cancer Cell Viability in Vitro

Wild type (wt) DuCaP prostate cancer cells endogenously express AKR1C3.^[36] Gene expression results reveal 27-fold AKR1C3 expression compared to AKR1C1, and 96-fold AKR1C3 expression compared to AKR1C2 (of which expression is negligible).^[38] Growth curves for DuCaP cells exposed to various compounds and androgen precursor over 10 days were measured by cell counting in a Biotek plate reader. DuCaP cells exposed to 1 nM 4-androstene-3,17-dione (Δ 4An), the natural substrate of AKR1C3 at physiologically relevant concentrations, showed increased proliferation as expected due to increased production of androgens by AKR1C3 that drive cell proliferation. Indomethacin, a selective AKR1C3 inhibitor, is known to inhibit the formation of testosterone from Δ 4An in LNCaP-AKR1C3 cells at 30 μM concentration.^[39] Hence, indomethacin was used as a positive control. Treatment of DuCaP cells with **3c**, a proline *N,N*-diethyl amide derivative and the most potent analogue identified (AKR1C3 IC₅₀ = 40 nM, AKR1C2 IC₅₀ = 100 nM) inhibited cell growth over 10 days in the presence of a physiologically relevant concentration of Δ 4An, showing the compound blocks the effect of the natural substrate (Figure 4A). An effect that can be attributed to the AKR1C3 inhibition activity of this compound given the negligible expression of AKR1C2 in these

cell lines. Given that AKR1C2 inhibition would prevent the metabolism of 5 α -dihydroxytestosterone this would be expected to counter the effect of inhibiting AKR1C3, thus a selective AKR1C3 inhibitor, such as indomethacin would be more potent to reduce proliferation. In AKR1C3 null LNCaP prostate cancer cells compounds **3a** (Figure 4B) and **3c** (Figure 4C) showed no effect to reduce cell viability up to 100 μM concentration. Likewise in non-malignant WPMY-1 prostate stromal cells no effect on cell viability is observed for compound **3a** (Figure 4D) or **3c** (Figure 4E) up to 100 μM concentration. Together this data suggests no adverse off-target effects.

Radiosensitization Effect

Literature reports indicate that AKR1C3 overexpression increases radiation resistance in human prostate cancer cells.^[22] Likewise, radiation-resistant esophageal carcinoma cell lines, KY170R and TE13R, showed increased AKR1C3 expression. Methyl jasmonate, a pan AKR1 family inhibitor,^[40] was reported to enhance the sensitivity of these cells to irradiation in clonogenic survival assays by inhibiting AKR1C3.^[20, 23] To determine the effect of our coumarin amide pan-AKR1C inhibitor to induce radiation sensitivity, we tested compound **3a** (AKR1C3 IC₅₀ = 50 nM, AKR1C2 IC₅₀ = 90 nM) at 10 μM concentration (Figure 5A) and the recently reported highly selective AKR1C3 inhibitor **5r** (designated as **K90**) (AKR1C3 IC₅₀ = 51 nM, AKR1C2 IC₅₀ = 62 μM)^[17] at an equal concentration of 10 μM (Figure 5B) in wild-type 22Rv1 human prostate cancer cells,^[41] which were irradiated with 2 Gy of X-rays and plated for a clonogenic survival assay. Cell culture was continued for 14 days, and the resulting colonies were then stained with crystal violet/methanol solution and enumerated using a dissecting microscope. Compounds **3a** and **K90** did not show significant radiosensitization effect in the 22Rv1 cells over that of corresponding DMSO controls (Mann-Whitney test).

Synergistic Effect in Primary Patient-Derived T-ALL and B-ALL Cells

Prior literature reports that a pan-AKR1C inhibitor, medroxyprogesterone acetate (MPA), tested in combination with bezafi-

Table 2. AKR1C3 and AKR1C2 IC₅₀* values of coumarin derivatives 2a–2f, and 3–5.

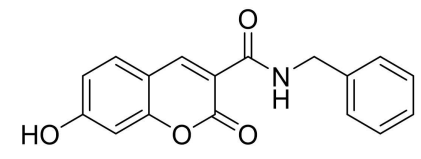
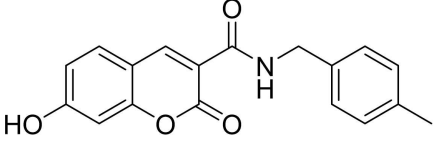
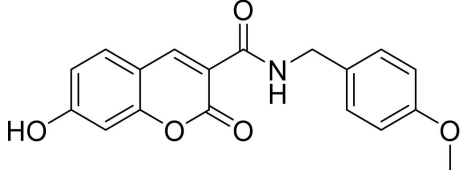
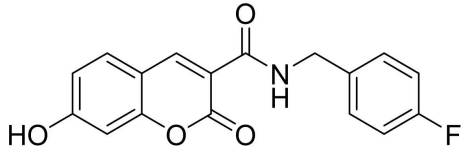
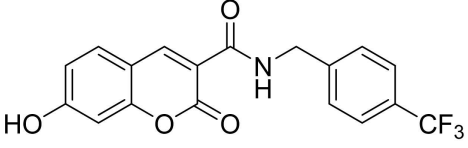
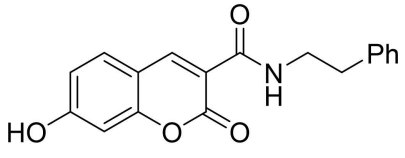
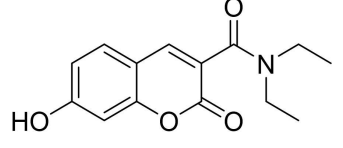
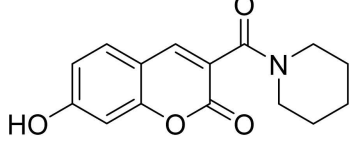
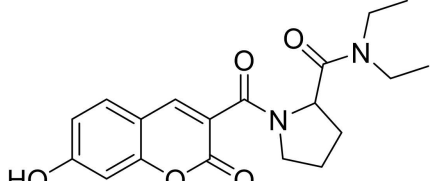
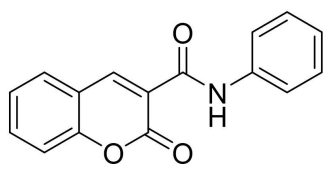
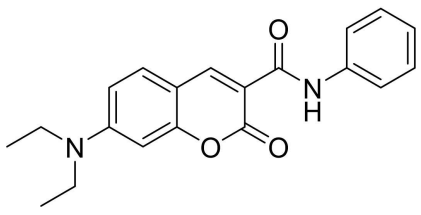
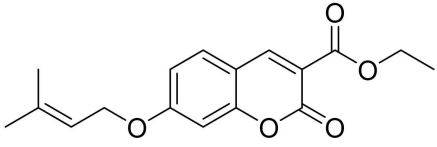
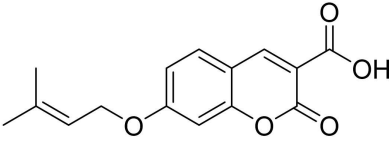
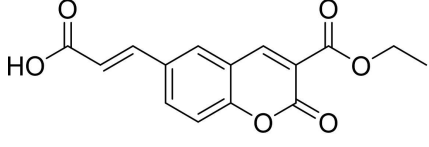
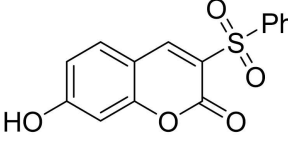
No.	Compound	AKR1C3 IC ₅₀ * (μM)	AKR1C2 IC ₅₀ * (μM)
2a		0.16 ± 0.02	ND ^[a]
2b		0.07 ± 0.00	0.07 ± 0.01
2c		0.17 ± 0.03	ND
2d		0.06 ± 0.08	0.10 ± 0.01
2e		0.09 ± 0.02	0.13 ± 0.01
2f		0.06 ± 0.00	0.08 ± 0.00
3a		0.05 ± 0.00	0.09 ± 0.01
3b		0.05 ± 0.00	0.09 ± 0.01
3c		0.04 ± 0.01	0.10 ± 0.00
3d		47.80 ± 4.60	ND

Table 2. continued			
No.	Compound	AKR1C3 IC ₅₀ * (μM)	AKR1C2 IC ₅₀ * (μM)
3e		19.13 ± 2.80	ND
4a		5.37 ± 0.84	1.60 ± 0.09
4b		1.09 ± 0.15	1.09 ± 0.17
4c		2.78 ± 0.49	ND
5		0.122 ± 0.009	0.139 ± 0.025

*Values represent the mean ± SEM of n = 3 experiments. ^[a] ND = not determined.

brate in human promyelocytic leukemia cell line, HL-60, human promyeloblast macrophage cell line, KG1a, and human chronic myelogenous leukemia cell line, K562, and primary patient chronic lymphocytic leukemia (CLL) cells, obtained from patients diagnosed with CLL at Birmingham Heartlands Hospital in the United Kingdom, induced anti-leukemic actions. However, when several *selective* AKR1C3 inhibitors were combined with bezafibrate this action was *not* observed.^[18] Increased AKR1C3 expression has been noted in patient-derived T-Cell acute lymphoblastic leukemia (T-ALL) and B-Cell acute lymphoblastic leukemia (B-ALL) cells, with expression higher in the T-ALL samples.^[9] Further, AKR1C1, -1C2 and -1C3 have been further reported to be overexpressed in pediatric T-ALL cell lines where chemotherapy induced activation of the enzymes.^[19] Treatment with the pan-AKR1C inhibitor MPA, sensitized three separate T-cell ALL cell lines (CCRF-CEM, DND-41 and LOUCY) to vincristine, *in vitro*, but not daunorubicin, cytarabine or *L*-asparaginase.^[19] Our prior studies have demonstrated that highly selective AKR1C3 inhibitors sensitized three human AML cell lines, and two recently-established human T-ALL cell lines to the cytotoxicity of etoposide,^[7] daunorubicin, and cytarabine, *in vitro*.^[5]

We determined the ability of pan-AKR1C inhibitor **3a** to sensitize a recently-established human patient-derived T-cell ALL cell line, COG-LL-317h, and human patient-derived pre-B-cell ALL cell line, TX-LL-057h, to the Bcl-2 inhibitor, ABT-737 (analogue of ABT-263, Navitoclax), daunorubicin, and dexamethasone using a sensitive *in vitro* cytotoxicity assay (DIMSCAN assay)^[42] (Figure 6). Compound **3a** failed to induce cytotoxicity as a single agent, or cytotoxic synergism in combination with ABT-737, daunorubicin or dexamethasone, in either cell line (Figure 6A and B). In contrast, the highly selective AKR1C3 inhibitor **K90**,^[17] while lacking cytotoxicity as a single agent, increased cytotoxicity in combination with both ABT-737 and daunorubicin, but not dexamethasone (Figure 6C). Both compounds **K90** and **3a** are equipotent to inhibit AKR1C3 (IC₅₀ = 50 nM), differing only in their selectivity to AKR1C1/2. Thus, potency did not appear to be a factor in the observed difference in the potentiation effects of **3a** and **K90**.

Conclusions

In summary, we have identified several 7-hydroxy coumarin benzyl and aliphatic amides as nanomolar pan-inhibitors of

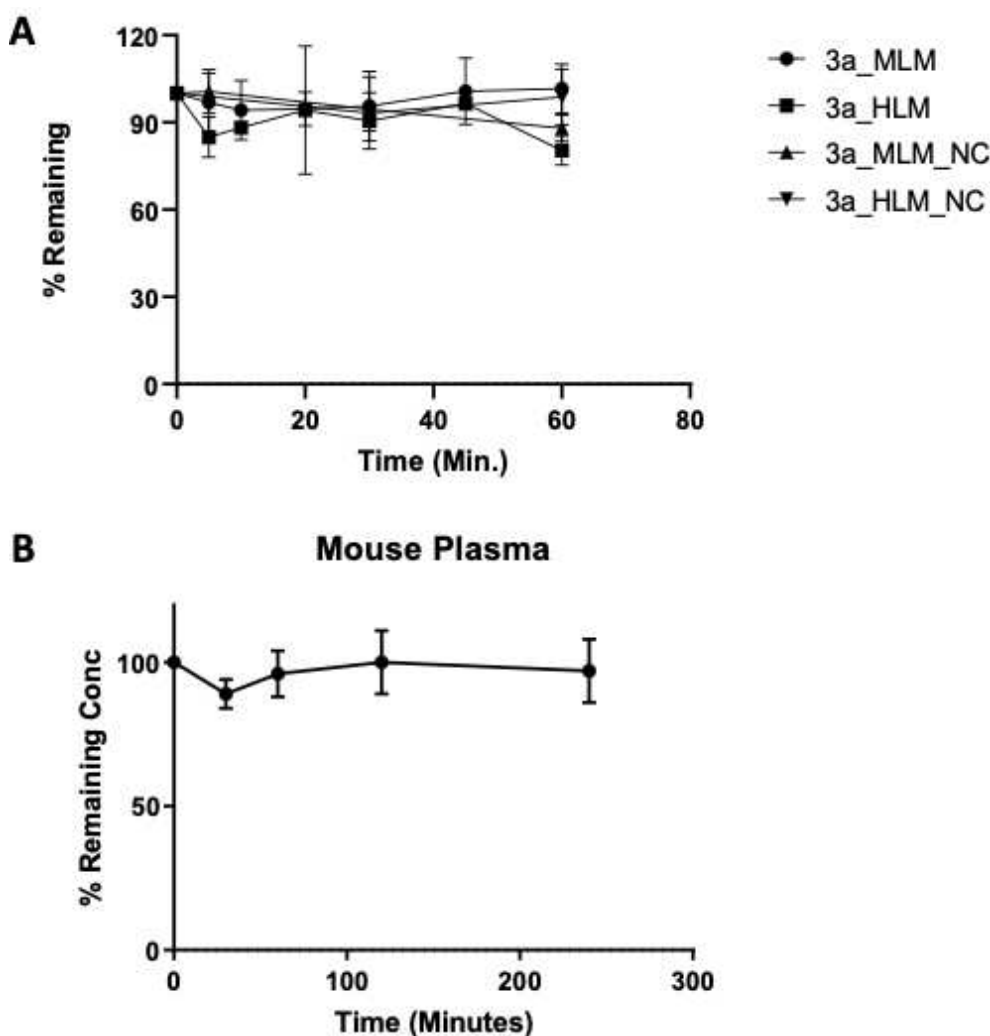


Figure 3. A) *In-vitro* metabolism of **3a** in mouse (MLM) and human liver microsomes (HLM), values represent the mean \pm SEM of $n = 3$ experiments. NC = negative control (without NADPH). B) *In-vitro* mouse plasma stability of **3a**, values represent the mean \pm SD of $n = 3$ experiments.

AKR1C family enzymes, identifying the 7-hydroxy and benzylamide moieties as pharmacophoric. These compounds exhibit 'drug-like' *in vitro* metabolic stability and half-life in human and mouse liver microsomes and plasma.

Coumarin amide **3c**, decreased cell proliferation of wt DuCaP prostate cancer cells in a highly relevant translational environment in the presence of 1 nM $\Delta 4$ An. It should be noted that the expression level of AKR1C2 in this cell line is negligible compared to the expression of AKR1C3. Thus, the observed effect to reduce cell count can be attributed to purely AKR1C3 inhibition. In prostate cancer cells that do express AKR1C2 and/or AKR1C1, a pan-AKR1C inhibitor would prevent the metabolism of 5 α -dihydrotestosterone which would counter the effect of inhibiting AKR1C3, thus pointing to the requirement of AKR1C3 selective inhibitors as potential treatments for prostate cancer.

Coumarin amide **3a** was tested for its ability to sensitize 22Rv1 prostate cancer cells to the effects of radiation, given the link between AKR1C3 expression and radiation resistance. By the method of assay used, the pan-AKR1C inhibitor did not

show appreciable radiation sensitization compared to controls, neither did the selective AKR1C3 inhibitor **K90**. Further investigation of radiosensitization and selectivity to AKR1C family members across prostate cancer cell lines is warranted.

No enhancement of cytotoxicity was observed when the pan-AKR1C inhibitor **3a** was tested in combination with the pan-BCL2 family inhibitor ABT-737, daunorubicin (an anthracycline), or the glucocorticoid dexamethasone, in two recently established human ALL cell lines. This result agrees with other reports on the effects of pan-AKR1C inhibitors combined with daunorubicin. In contrast, potentiation was observed when a selective AKR1C3 inhibitor, **K90**, was combined with ABT-737 or daunorubicin. The cytotoxic effects of dexamethasone were not affected by either the selective or pan-inhibitor, suggesting that glucocorticoid resistance may be AKR-independent. Both previous reports on the effect of combining pan-AKR1C inhibitors with bezafibrate or vincristine, and the results reported herein, suggest that the specific requirement needed to effect cytotoxic enhancement of chemotherapy agents, i.e, either a pan- or AKR1C3-selective inhibitor, is chemotherapy agent dependent

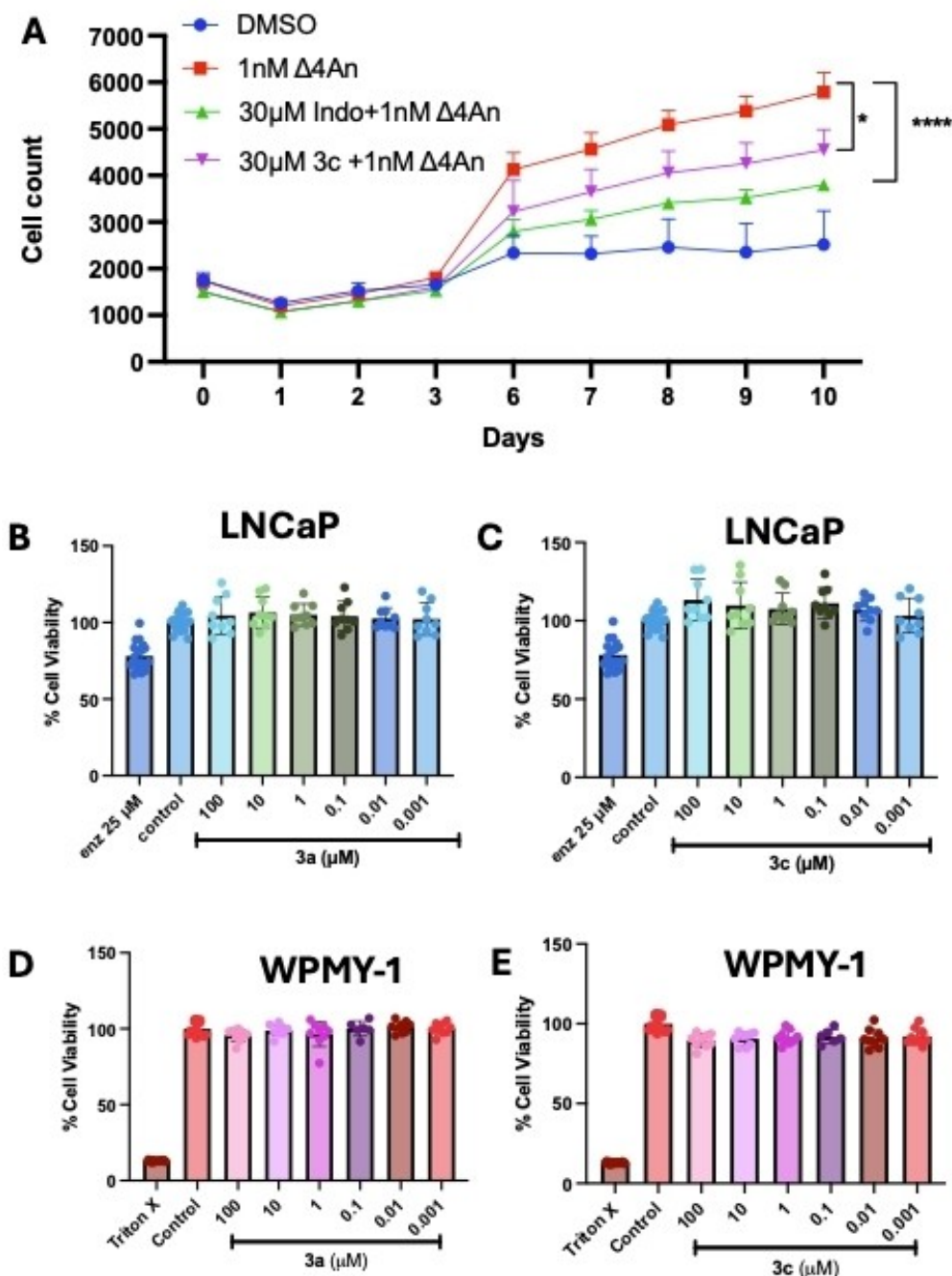


Figure 4. Effect of compounds **3a** and **3c** on cell proliferation. A) AKR1C3 expressing DuCap Wt cells in the presence of 1 nM Δ 4An, 30 μ M **3c** or indomethacin (Indo). B) AKR1C3 null LNCaP cells in the presence of **3a** at indicated concentrations. C) AKR1C3 null LNCaP cells in the presence of **3c** at indicated concentrations. D) WPMY-1 non-malignant prostate stromal cells in the presence of **3a** at indicated concentrations. E) WPMY-1 non-malignant prostate stromal cells in the presence of **3c** at indicated concentrations. Values represent the mean \pm SD of $n=3$ experiments. *, $p < 0.05$; ****, $p < 0.0001$ by two-way ANOVA.

and cancer cell type specific, supporting a role for precision approaches in chemotherapy regimens (Table 3) and requires further definition. This may be related to the structure of the chemotherapeutic and its ability to be recognized as a substrate by the various members of the AKR1C family.

Experimental Section

Chemistry

Solvents and reagents of commercial-grade were purchased from Fisher Scientific, VWR, Millipore-Sigma or AK Scientific and were used without additional purification. All reactions were performed in oven-dried flasks under nitrogen atmosphere. Reaction progress was monitored using thin-layer chromatography (TLC) on Alumi-

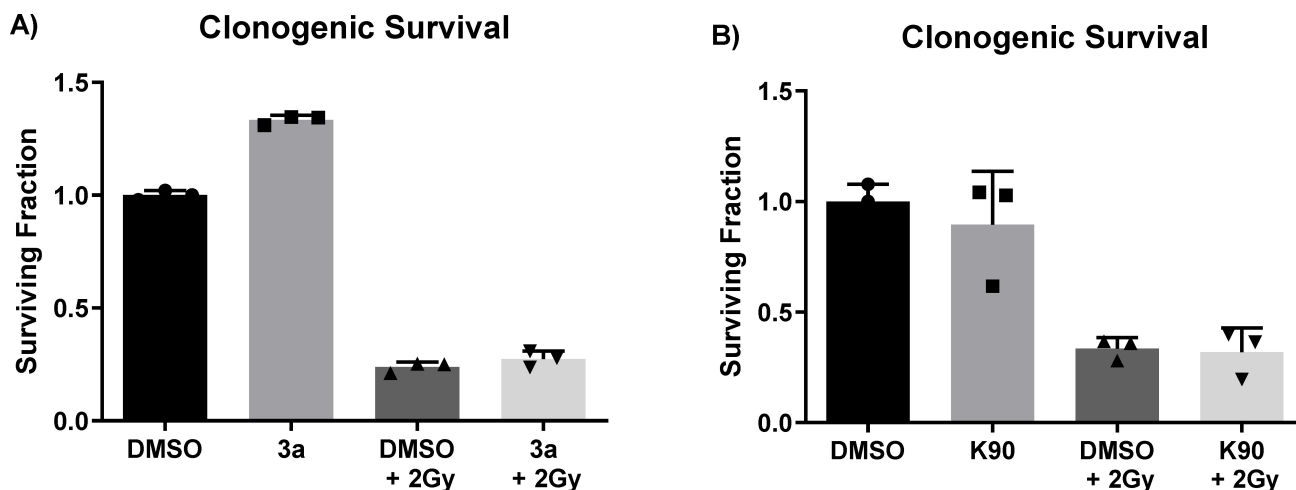


Figure 5. Clonogenic survival in 22Rv1 cells treated with A) 10 μM **3a** and B) 10 μM **K90** and then irradiated with 2 Gy X-rays. Values represent the mean \pm SD of $n=3$ experiments.

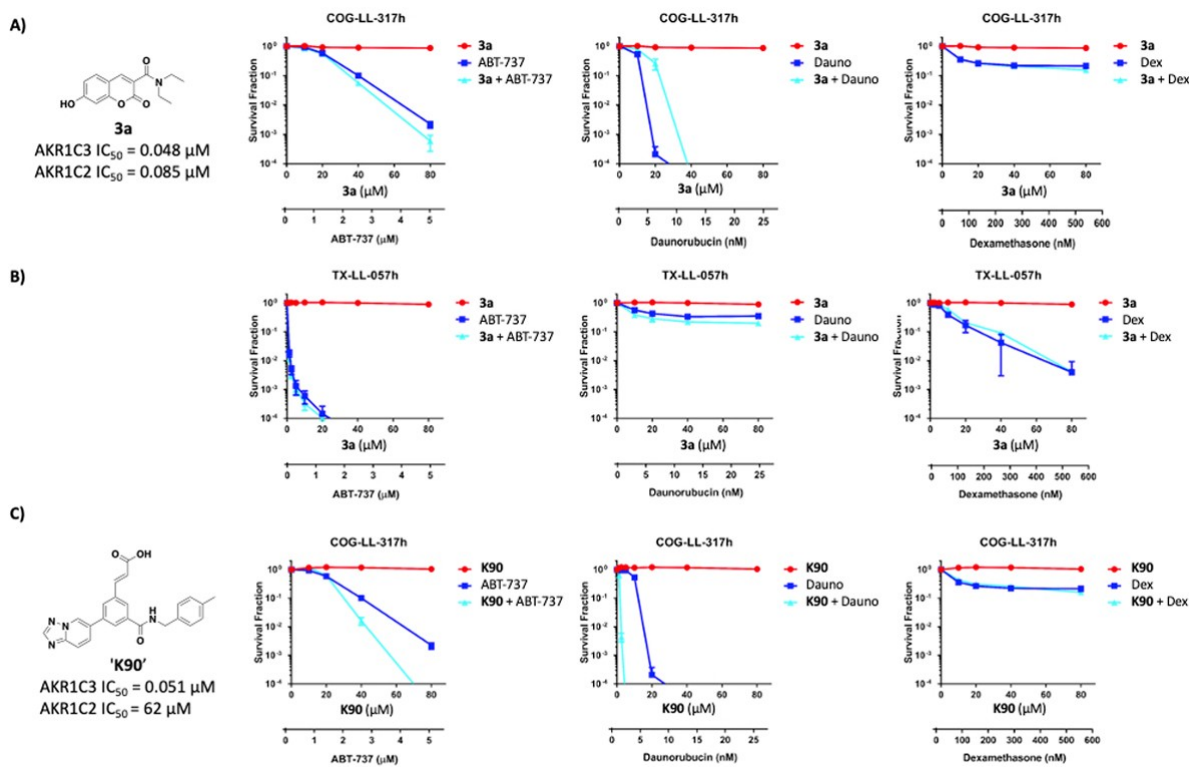


Figure 6. Selective AKR1C3 inhibitor, **K90**, but not pan-AKR1C inhibitor, **3a**, potentiated the cytotoxicity of ABT-737 and daunorubicin in patient-derived ALL leukemia cell lines, *in vitro*. A, B) Structure, and cytotoxic dose-response, of **3a**, alone and in combination with ABT-737, daunorubicin, or dexamethasone in the COG-LL-317h T-cell ALL and TX-LL-057h pre-B-cell ALL cell lines. C) Structure, and cytotoxic dose-response of **K90**, alone and in combination with ABT-737, daunorubicin, or dexamethasone in COG-LL-317h T-cell ALL cells. Cytotoxicity assayed using DIMSCAN assay. Values represent the mean \pm SEM of $n=2$ experiments performed in triplicate.

nium-backed 20 μm silica plates (Silicycle, TLA-R1001B-323) and visualized by UV (254 nm) or staining agent (ninhydrin solution, phosphomolybdic acid or iodine vapor). Flash column chromatography was performed on silica gel (40–63 μm , 60 \AA) with the indicated mobile phase.

NMR spectrometric analysis was carried out using the indicated solvent on a Bruker Avance III HD spectrometer at 400, 500 or 600 MHz for proton (^1H) and 100, 126 or 150 MHz for carbon (^{13}C),

respectively. Chemical shifts (δ) are recorded in parts per million (ppm) and reported relative to solvents; coupling constants (J) are reported in hertz (Hz). Splitting of signal peaks are indicated by s (singlet), d (doublet), dd (doublet of doublets), t (triplet), q (quartet), m (multiplet), and br (broad). High-resolution mass spectrometry (HRMS) was carried out on an Agilent 1200 time-of-flight mass spectrometer equipped with an electrospray ionization source. HPLC purity data for all final compounds were performed on a Waters ACQUITY ultra-performance liquid chromatography (UPLC)

Table 3. Summary of AKR1C family inhibition profile required to confer cytotoxicity enhancement in combination with indicated chemotherapeutics in leukemia cell models.

Chemotherapeutic	Cell Line	Required AKR1C family inhibition profile	Reference
Bezafibrate	HL-60, K562, KG1a, Primary CLL	Promiscuous	[4]
Vincristine	Primary T-ALL	Promiscuous	[5]
Etoposide	HL-60, KG1a	AKR1C3 selective	[3c]
Daunorubicin	HL-60, KG1a, THP-1, COG-LL-317h	AKR1C3 selective	[3a,5], Herein
Cytarabine	HL-60, KG1a, THP-1, COG-LL-317h	AKR1C3 selective	[3a,5]
ABT-737	COG-LL-317h, TX-LL-057h	AKR1C3 selective	Herein
Dexamethasone	COG-LL-317h, TX-LL-057h	Neither AKR1C3 selective nor promiscuous	Herein

H-Class System with TUV (254 nm) detector and Empower 2 software (Milford, MA, USA) using an Agilent Eclipse plus C18 5 μ column (4.6x150 mm). All compounds were evaluated to be of $\geq 95\%$ purity.

General method for the synthesis of compounds 1a–1i: 4-Methoxy salicylaldehyde (2 g, 16.38 mmol), diethylmalonate (3.94 g, 24.57 mmol) and piperidine (279 mg, 3.28 mmol) were stirred at 50 °C overnight. Upon completion of the reaction, water was added to the mixture and stirred for 10 minutes. The resulting solid was filtered and washed with water followed by hexanes and the crude product was recrystallized in ethyl acetate to afford **1c**. To a suspension of **1c** (440 mg, 1.77 mmol) in 5 mL water, NaOH (142 mg, 3.55 mmol) was added, and the reaction mixture was stirred at 50 °C for 12 hours. The reaction was cooled to room temperature, quenched with ice-cold 3 N HCl, filtered and washed with water and hexanes. The crude product was purified via recrystallization in EtOAc-hexanes to obtain coumarin carboxylic acid **1h**.

Ethyl 2-oxo-2H-chromene-3-carboxylate (1a): 3.2 g (90% yield), off white solid. ^1H NMR (400 MHz, CDCl_3): δ 8.53 (s, 1H), 7.38–7.62 (m, 2H), 7.38–7.333 (m, 2H), 4.42 (q, $J=7.2$ Hz, 2H), 1.42 (t, $J=7.2$ Hz, 3H). ^{13}C NMR (100 MHz, CDCl_3): δ 163.1, 156.7, 155.2, 148.6, 134.3, 129.5, 124.8, 118.4, 117.9, 116.8, 62.0, 14.2. HRMS-ESI (m/z): $[\text{M} + \text{H}]^+$: calc. for $\text{C}_{12}\text{H}_{11}\text{O}_4$ 219.0652, found 219.0647.

Ethyl 7-methyl-2-oxo-2H-chromene-3-carboxylate (1b): 1.7 g (99% yield), off white solid. ^1H NMR (500 MHz, $\text{DMSO}-d_6$): δ 8.72 (s, 1H), 7.81 (d, $J=8.0$ Hz, 1H), 7.29–7.24 (m, 2H), 4.30 (q, $J=7.0$ Hz, 2H), 2.45 (s, 3H), 1.31 (t, $J=7.0$ Hz, 3H). ^{13}C NMR (125 MHz, $\text{DMSO}-d_6$): δ 163.2, 156.6, 155.2, 149.3, 146.5, 130.5, 126.5, 116.8, 116.7, 115.9, 61.6, 22.0, 14.6. HRMS-ESI (m/z): $[\text{M} + \text{H}]^+$: calc. for $\text{C}_{13}\text{H}_{13}\text{O}_4$ 233.0809, found 233.0814.

Ethyl 7-methoxy-2-oxo-2H-chromene-3-carboxylate (1c): 2.9 g (77% yield), off white solid. ^1H NMR (400 MHz, CDCl_3): δ 8.50 (s, 1H), 7.51 (d, $J=8.8$ Hz, 1H), 6.91–6.88 (m, 1H), 6.81 (s, 1H), 4.40 (q, $J=7.2$ Hz, 2H), 3.91 (s, 3H), 1.41 (t, $J=7.2$ Hz, 3H). ^{13}C NMR (100 MHz, CDCl_3): δ 165.1, 163.4, 157.6, 157.1, 148.9, 130.7, 114.2, 113.6, 111.6, 100.4, 61.7, 56.0, 14.3. HRMS-ESI (m/z): $[\text{M} + \text{H}]^+$: calc. for $\text{C}_{13}\text{H}_{13}\text{O}_5$ 249.0758, found 249.0760.

Ethyl 7-fluoro-2-oxo-2H-chromene-3-carboxylate (1d): 3.2 g (95% yield), pale yellow solid. ^1H NMR (500 MHz, $\text{DMSO}-d_6$): δ 8.79 (s, 1H), 8.04–8.01 (m, 1H), 7.46 (dd, $J=9.5, 2.5$ Hz, 1H), 7.35–7.31 (m, 1H), 4.30 (q, $J=7.0$ Hz, 2H), 1.31 (t, $J=7.0$ Hz, 3H). ^{13}C NMR (125 MHz, $\text{DMSO}-d_6$): δ 166.9, 156.6, 156.5, 156.2, 148.9, 133.2, 133.1, 116.9, 115.5, 113.6, 113.4, 104.5, 104.3, 61.7, 14.6. HRMS-ESI (m/z): $[\text{M} + \text{H}]^+$: calc. for $\text{C}_{12}\text{H}_{10}\text{FO}_4$ 237.0558, found 237.0535.

Ethyl 7-bromo-2-oxo-2H-chromene-3-carboxylate (1e): 1.4 g (63% yield), white solid. ^1H NMR (500 MHz, $\text{DMSO}-d_6$): δ 8.76 (s, 1H), 7.87 (d, $J=8.0$ Hz, 1H), 7.79 (s, 1H), 7.62 (d, $J=7.0$ Hz, 1H), 4.30 (q, $J=7.0$ Hz, 2H), 1.31 (t, $J=7.5$ Hz, 3H). ^{13}C NMR (125 MHz, $\text{DMSO}-d_6$): δ 162.9, 156.1, 155.3, 148.6, 132.1, 128.5, 128.1, 119.7, 118.4, 117.6, 61.8, 14.5. HRMS-ESI (m/z): $[\text{M} + \text{H}]^+$: calc. for $\text{C}_{12}\text{H}_{10}\text{BrO}_4$ 296.9757, found 296.9750.

Ethyl 7-hydroxy-2-oxo-2H-chromene-3-carboxylate (1f): 3.1 g (90% yield), pale brown solid. ^1H NMR (500 MHz, $\text{DMSO}-d_6$): δ 11.08 (s, 1H), 8.67 (s, 1H), 7.76 (d, $J=8.5$ Hz, 1H), 6.85 (dd, $J=8.5, 2.0$ Hz, 1H), 6.73 (d, $J=2.5$ Hz, 1H), 4.26 (q, $J=7.0$ Hz, 2H), 1.30 (t, $J=7.5$ Hz, 3H). ^{13}C NMR (125 MHz, $\text{DMSO}-d_6$): δ 164.5, 163.4, 157.6, 156.9, 149.9, 132.6, 114.5, 112.6, 110.9, 102.3, 61.3, 14.6. HRMS-ESI (m/z): $[\text{M} + \text{H}]^+$: calc. for $\text{C}_{12}\text{H}_{11}\text{O}_5$ 235.0601, found 235.0611.

Ethyl 7-(diethylamino)-2-oxo-2H-chromene-3-carboxylate (1g): 3.6 g (80% yield), greenish yellow solid. ^1H NMR (500 MHz, $\text{DMSO}-d_6$): δ 8.54 (s, 1H), 7.62 (d, $J=9.0$ Hz, 1H), 6.77 (d, $J=9.0$ Hz, 1H), 6.53 (s, 1H), 4.23 (q, $J=7.0$ Hz, 2H), 3.48 (q, $J=7.0$ Hz, 4H), 1.28 (t, $J=7.0$ Hz, 3H), 1.14 (t, $J=7.0$ Hz, 6H). ^{13}C NMR (125 MHz, $\text{DMSO}-d_6$): δ 163.9, 158.5, 157.5, 153.3, 149.7, 132.2, 110.2, 107.9, 107.5, 96.3, 60.8, 44.8, 14.7, 12.8. HRMS-ESI (m/z): $[\text{M} + \text{H}]^+$: calc. for $\text{C}_{16}\text{H}_{20}\text{NO}_4$ 290.1387, found 290.1410.

7-methoxy-2-oxo-2H-chromene-3-carboxylic acid (1h): 1.5 g (68% yield), white solid. ^1H NMR (400 MHz, $\text{DMSO}-d_6$): δ 8.69 (s, 1H), 7.48 (d, $J=2.5$ Hz, 1H), 7.40 (d, $J=8.9$ Hz, 1H), 7.33 (dd, $J=8.8, 2.5$ Hz, 1H), 3.81 (s, 3H). ^{13}C NMR (100 MHz, $\text{DMSO}-d_6$): δ 164.4, 157.4, 156.2, 149.4, 148.5, 122.4, 119.0, 118.8, 117.7, 112.3, 56.3. HRMS-ESI (m/z): $[\text{M} + \text{Na}]^+$: calc. for $\text{C}_{11}\text{H}_9\text{O}_5$ 243.1673, found: 243.1631. HRMS-ESI (m/z): $[\text{M} + \text{H}]^+$: calc. for $\text{C}_{11}\text{H}_9\text{O}_5$ 221.0445, found.

7-(diethylamino)-2-oxo-2H-chromene-3-carboxylic acid (1i): 1.8 g (70% yield), brick-red solid. ^1H NMR (500 MHz, $\text{DMSO}-d_6$): δ 12.44 (br s, 1H), 8.59 (s, 1H), 7.64 (d, $J=9.0$ Hz, 1H), 6.80 (dd, $J=9.0, 2.5$ Hz, 1H), 6.57 (d, $J=2.5$ Hz, 1H), 3.49 (q, $J=7.0$ Hz, 4H), 1.14 (t, $J=7.0$ Hz, 6H). ^{13}C NMR (125 MHz, $\text{DMSO}-d_6$): δ 165.0, 160.0, 158.4, 153.4, 149.9, 132.3, 110.5, 107.8, 107.6, 96.4, 44.9, 12.8. HRMS-ESI (m/z): $[\text{M} + \text{H}]^+$: calc. for $\text{C}_{14}\text{H}_{16}\text{NO}_4$ 262.1074, found 262.1073.

6-hydroxy-2-oxo-2H-chromene-3-carboxylic acid (1k): 1.5 g (68% yield), white solid. ^1H NMR (600 MHz, $\text{DMSO}-d_6$): δ 12.88 (br s, 1H), 11.06 (s, 1H), 8.68 (s, 1H), 7.74 (d, $J=8.4$ Hz, 1H), 6.84 (dd, $J=9.0, 2.4$ Hz, 1H), 6.73 (d, $J=1.8$ Hz, 1H). ^{13}C NMR (150 MHz, $\text{DMSO}-d_6$): δ 164.7, 164.4, 158.0, 157.5, 149.9, 132.5, 114.5, 112.9, 111.1, 102.3. HRMS-ESI (m/z): $[\text{M} + \text{H}]^+$: calc. for $\text{C}_{10}\text{H}_7\text{O}_5$ 207.0288, found 207.0236.

Synthesis of ethyl 7-amino-2-oxo-2H-chromene-3-carboxylate (1j): To a solution of **1e** (1 g, 3.37 mmol) in 5 mL DMSO, sodium azide (263 mg, 4.04 mmol) was added, and the reaction was heated at

80 °C for 4 hours. The reaction mixture was poured into ice-cold water and the resulting solid was filtered and washed with water and hexanes to obtain azide intermediate, which was used in the next step without further purification. The azide was dissolved in 5 mL methanol and 10% Pd/C (90 mg, 0.85 mmol) was added. Hydrogen gas was filled in a balloon and the reaction mixture was exposed to hydrogen at room temperature for 1 hour. The reaction was filtered on celite and washed with methanol and evaporated to obtain crude product, which was purified via column chromatography (DCM 95%, 5% MeOH) to afford 7-amino coumarin carboxylic acid ethyl ester **1j**. Pale yellow solid (288 mg, 37% yield). ¹H NMR (500 MHz, DMSO-*d*₆): δ 8.51 (s, 1H), 7.52 (d, *J* = 8.5 Hz, 1H), 6.80 (br s, 2H), 6.39 (s, 1H), 4.22 (q, *J* = 7.0 Hz, 2H), 1.28 (t, *J* = 7.0 Hz, 3H). ¹³C NMR (125 MHz, DMSO-*d*₆): δ 163.9, 158.6, 157.4, 156.7, 150.0, 132.5, 112.7, 107.9, 107.7, 97.9, 60.8, 14.7. HRMS-ESI (*m/z*): [M + H]⁺: calc. for C₁₂H₁₂NO₄ 234.0761, found 234.0764.

General procedure for the synthesis of coumarin amides 2a–2f: To a suspension of 7-hydroxy coumarin carboxylic acid ethyl ester **1f** (4.0 g, 17.1 mmol) in 5 mL THF and water (1:1), NaOH (2.73 g, 68.3 mmol) was added, and the reaction was heated at 50 °C overnight. The reaction mixture was quenched with ice-cold dilute HCl and the resulting solid was filtered and washed with water and hexanes to obtain 7-hydroxy coumarin carboxylic acid, which was used in the next reaction without further purification. To a stirred solution of 7-hydroxy coumarin carboxylic acid (1 g, 4.85 mmol) in DMF (5 mL), acetic anhydride (7.32 mL, 77.61 mmol) was added, and the reaction mixture was heated overnight at 50 °C. Upon completion, the reaction was poured in water and the resulting solid was filtered and washed with water and hexanes, and dried to obtain 7-acetyl coumarin acid **1l** (950 mg, 79% yield), which was used in the next reaction without further purification. To a solution of 7-acetyl coumarin carboxylic acid (250 mg, 1.01 mmol) in 10 mL of DCM and DMF (1:1), EDC.HCl (193 mg, 1.01 mmol) and HOBt (154 mg, 1.01 mmol) was added, and the reaction was stirred at room temperature for 10–15 minutes. To this reaction mixture, benzyl amine (108 mg, 1.01 mmol) was added followed by the addition of triethylamine (0.42 mL, 3.02 mmol) and the reaction was heated at 50 °C overnight. After completion of the reaction, the solution was quenched with 3 N HCl followed by aqueous NaOH and extracted with DCM. The organic layer was separated, dried with anhydrous sodium sulfate, and evaporated under vacuum. The crude product was purified by flash column chromatography using 10% MeOH/DCM as eluent to afford the corresponding coumarin amide.

7-acetoxy-2-oxo-2H-chromene-3-carboxylic acid (1l): Off white solid (950 mg, 79% yield). ¹H NMR (400 MHz, DMSO-*d*₆): δ 8.75 (s, 1H), 7.95 (d, *J* = 8.4 Hz, 1H), 7.31 (s, 1H), 7.21 (dd, *J* = 8.4 Hz, 2.0 Hz, 1H), 2.32 (s, 3H). ¹³C NMR (100 MHz, DMSO-*d*₆): δ 169.1, 164.4, 156.9, 155.7, 155.2, 148.5, 131.7, 119.5, 117.9, 116.3, 110.3, 21.4.

N-benzyl-7-hydroxy-2-oxo-2H-chromene-3-carboxamide (2a): Beige solid (180 mg, 60.5% yield). ¹H NMR (400 MHz, DMSO-*d*₆): δ 9.05 (t, *J* = 6.0 Hz, 1H), 8.81 (s, 1H), 7.82 (d, *J* = 8.6 Hz, 1H), 7.34 (d, *J* = 4.1 Hz, 4H), 7.28–7.25 (m, 1H), 6.88 (dd, *J* = 8.6 Hz, 2.1 Hz, 1H), 6.81 (s, 1H), 4.54 (d, *J* = 6.0 Hz, 2H). ¹³C NMR (100 MHz, DMSO-*d*₆): δ 164.1, 162.2, 161.5, 156.8, 148.6, 139.5, 132.5, 128.9, 127.8, 127.4, 114.8, 114.2, 111.6, 102.3, 43.1. HRMS-ESI (*m/z*): [M + H]⁺: calc. for C₁₇H₁₄NO₄ 296.0918, found 296.0918.

7-hydroxy-N-(4-methylbenzyl)-2-oxo-2H-chromene-3-carboxamide (2b): Beige solid (210 mg, 67% yield). ¹H NMR (400 MHz, DMSO-*d*₆): δ 8.99 (t, *J* = 6.0 Hz, 1H), 8.82 (s, 1H), 7.82 (d, *J* = 8.8 Hz, 1H), 7.22 (d, *J* = 8.0 Hz, 2H), 7.14 (d, *J* = 8.0 Hz, 2H), 6.88 (dd, *J* = 8.4 Hz, 2.4 Hz, 1H), 6.81 (s, 1H), 4.48 (d, *J* = 5.8 Hz, 1H), 2.27 (s, 3H). ¹³C NMR (100 MHz, DMSO-*d*₆): δ 164.2, 162.1, 161.5, 156.8, 148.6, 136.5, 136.4,

132.5, 129.4, 127.9, 114.8, 114.1, 111.6, 102.3, 42.9, 21.1. HRMS-ESI (*m/z*): [M + H]⁺: calc. for C₁₈H₁₆NO₄ 310.1074, found 310.1074.

7-hydroxy-N-(4-methoxybenzyl)-2-oxo-2H-chromene-3-carboxamide (2c): Beige solid (235 mg, 72% yield). ¹H NMR (400 MHz, DMSO-*d*₆): δ 8.97 (t, *J* = 6.0 Hz, 1H), 8.80 (s, 1H), 7.82 (d, *J* = 8.8 Hz, 1H), 7.27 (d, *J* = 8.65 Hz, 2H), 6.92–6.87 (m, 3H), 6.80 (s, 1H), 4.45 (d, *J* = 6.0 Hz, 2H), 3.73 (s, 3H). ¹³C NMR (100 MHz, DMSO-*d*₆): δ 164.2, 162.0, 161.5, 158.8, 156.8, 148.6, 132.5, 131.4, 129.3, 114.8, 114.3, 114.1, 111.6, 102.3, 55.5, 42.6. HRMS-ESI (*m/z*): [M + H]⁺: calc. for C₁₈H₁₆NO₅ 326.1023, found 326.1025.

N-(4-fluorobenzyl)-7-hydroxy-2-oxo-2H-chromene-3-carboxamide (2d): Beige solid (242 mg, 77% yield). ¹H NMR (500 MHz, DMSO-*d*₆): δ 11.08 (s, 1H), 9.08 (t, *J* = 5.8 Hz, 1H), 8.80 (s, 1H), 7.82 (d, *J* = 8.6 Hz, 1H), 7.39 (d, *J* = 6.6 Hz, 2H), 7.16 (t, *J* = 8.6 Hz, 2H), 6.89 (d, *J* = 8.6 Hz, 1H), 6.81 (s, 1H), 4.51 (d, *J* = 6.0 Hz, 2H). ¹³C NMR (125 MHz, DMSO-*d*₆): δ 164.2, 162.7, 162.2, 161.4, 160.7, 156.8, 148.7, 135.9, 135.8, 132.5, 129.9, 129.9, 115.6, 115.5, 114.8, 114.2, 111.6, 102.3, 42.4. HRMS-ESI (*m/z*): [M + H]⁺: calc. for C₁₇H₁₃FNO₄ 314.0824, found 314.0857.

7-hydroxy-2-oxo-N-(4-(trifluoromethyl)benzyl)-2H-chromene-3-carboxamide (2e): Beige solid (231 mg, 63% yield). ¹H NMR (400 MHz, DMSO-*d*₆): δ 11.1 (br-s, 1H), 9.19 (t, *J* = 6.0 Hz, 1H), 8.80 (s, 1H), 7.82 (d, *J* = 8.4 Hz, 1H), 7.69 (d, *J* = 7.8 Hz, 2H), 7.55 (d, *J* = 7.8 Hz, 2H), 6.89 (d, *J* = 8.6 Hz, 1H), 6.82 (s, 1H), 4.62 (d, *J* = 6.0 Hz, 1H). ¹³C NMR (100 MHz, DMSO-*d*₆): δ 164.2, 162.5, 161.4, 156.8, 148.8, 144.7, 132.5, 128.4, 125.7, 125.6, 114.8, 114.1, 111.6, 102.3, 42.8. HRMS-ESI (*m/z*): [M + H]⁺: calc. for C₁₈H₁₃F₃NO₄ 364.0792, found 364.0811.

7-hydroxy-2-oxo-N-phenethyl-2H-chromene-3-carboxamide (2f): Beige solid (242 mg, 78% yield). ¹H NMR (400 MHz, DMSO-*d*₆): δ 11.08 (s, 1H), 8.89 (s, 1H), 8.71 (t, *J* = 5.0 Hz, 1H), 7.82 (d, *J* = 8.5 Hz, 1H), 7.32–7.20 (m, 5H), 6.89 (d, *J* = 8.5 Hz, 1H), 6.80 (s, 1H), 3.56 (q, *J* = 6.5 Hz, 2H), 2.84 (t, *J* = 7.0 Hz, 2H). ¹³C NMR (100 MHz, DMSO-*d*₆): δ 164.1, 161.9, 161.5, 156.7, 148.5, 139.7, 132.5, 129.1, 128.9, 126.7, 114.8, 114.0, 111.6, 102.3, 41.1, 35.5. HRMS-ESI (*m/z*): [M + H]⁺: calc. for C₁₈H₁₆NO₄ 310.1074, found 310.1074.

Synthesis of coumarin amides 3a-1 and 3a: In a solution of diethylamine (0.125 mL, 1.21 mmol) and triethylamine (0.421 mL, 3.02 mmol) in dichloromethane (10 mL), 7-acetyl carboxylic acid **1l** (250 mg, 1.01 mmol) was added, followed by the addition of SOCl₂ (120 mg, 1.01 mmol) at room temperature. The mixture is stirred for 5–20 minutes at room temperature. The solvents were evaporated under vacuum and the resulting residue is dissolved in DCM and extracted with water, half of the DCM layer was dried with anhydrous sodium sulfate and evaporated under vacuum to obtain the 7-acetyl coumarin diethyl amide **3a-1**, which was purified using column chromatography. The other half of the DCM layer was extracted with 4 N NaOH, and organic layer was separated and extracted with water. The DCM layer was dried using anhydrous sodium sulfate and evaporated under vacuum to obtain 7-hydroxy coumarin diethyl amide **3a**. The product was purified via column chromatography.

3-(diethylcarbamoyl)-2-oxo-2H-chromen-7-yl acetate (3a-1): Off white solid, yield (182 mg, 69% yield). ¹H NMR (500 MHz, DMSO-*d*₆): δ 7.81 (s, 1H), 7.55 (d, *J* = 7.5 Hz, 1H), 7.17 (d, *J* = 1.5 Hz, 1H), 7.11 (dd, *J* = 7.0, 1.5 Hz, 1H), 3.59–3.56 (m, 2H), 3.33–3.29 (m, 2H), 2.37 (s, 3H), 1.28 (t, *J* = 6.0 Hz, 3H), 1.20 (t, *J* = 6.0 Hz, 3H); ¹³C NMR (125 MHz, DMSO-*d*₆): δ 168.7, 164.2, 157.8, 154.6, 153.7, 140.8, 129.1, 125.7, 118.9, 116.2, 110.4, 43.3, 39.6, 21.1, 14.1, 12.8; HRMS-ESI (*m/z*): [M + H]⁺: calc. for C₁₆H₁₈NO₅ 304.1180, found 304.1179.

N,N-diethyl-7-hydroxy-2-oxo-2H-chromene-3-carboxamide (3a): Beige solid (182 mg, 69% yield). ¹H NMR (500 MHz, DMSO-*d*₆): δ 7.95 (s, 1H), 7.55 (d, *J* = 7.0 Hz, 1H), 6.85 (dd, *J* = 7.5, 2.0 Hz, 1H), 6.77 (d, *J* =

2.0 Hz, 1H), 3.58–3.54 (m, 2H), 3.39–3.35 (m, 2H), 1.27–1.18 (m, 6H); ^{13}C NMR (100 MHz, DMSO- d_6): δ 166.1, 162.7, 159.1, 156.0, 142.3, 130.0, 120.2, 113.7, 111.0, 102.0, 43.4, 39.5, 12.9, 11.5. HRMS-ESI (m/z): $[\text{M} + \text{H}]^+$: calc. for $\text{C}_{14}\text{H}_{16}\text{NO}_4$ 262.1074, found 262.1079.

Synthesis of 7-hydroxy-3-(piperidine-1-carbonyl)-2H-chromen-2-one (3b). To a solution of 7-acetyl coumarin carboxylic acid **11** (500 mg, 2.43 mmol) in 10 mL DCM and DMF (1:1), EDC.HCl (558 mg, 2.91 mmol) and DMAP (296 mg, 2.42 mmol) were added, and the reaction was stirred at room temperature for 10–15 minutes. To this reaction mixture, piperidine (0.24 mL, 2.43 mmol) was added and the reaction was heated at 50 °C overnight. Upon completion of the reaction, the solution was quenched with 3 N HCl followed by aqueous NaOH and extracted with DCM. The organic layer was separated, dried with anhydrous sodium sulfate, and evaporated under vacuum. The crude product was purified by flash column chromatography using 10% MeOH/DCM as eluent to afford the corresponding coumarin amide **3b**. Off white solid (326 mg, 49%). ^1H NMR (400 MHz, DMSO- d_6): δ 7.97 (s, 1H), 7.55 (d, $J=7.0$, 1H), 6.86 (dd, $J=7.0$, 1.5 Hz, 1H), 6.77 (d, $J=1.5$ Hz, 1H), 3.70 (t, $J=4.5$ Hz, 2H), 3.41 (t, $J=4.5$ Hz, 2H), 1.73–1.63 (m, 6H); ^{13}C NMR (100 MHz, DMSO- d_6): δ 164.8, 162.8, 159.0, 156.1, 143.1, 130.1, 119.8, 113.7, 111.1, 102.0, 48.3, 42.8, 25.9, 25.2, 24.0; HRMS-ESI (m/z): $[\text{M} + \text{H}]^+$: calc. for $\text{C}_{15}\text{H}_{16}\text{NO}_4$ 274.1074, found 274.1077.

Synthesis of *N,N*-diethyl-1-(7-hydroxy-2-oxo-2H-chromene-3-carbonyl)pyrrolidine-2-carboxamide (3c). In a solution of diethylamine (0.577 mL, 5.56 mmol) and triethylamine (1.94 mL, 13.94 mmol) in dichloromethane (20 mL), Boc-L-proline (1 g, 4.65 mmol) was added, followed by the addition of SOCl_2 (553 mg, 4.65 mmol) at room temperature. The mixture is stirred for 5–20 minutes at room temperature. The solvents were evaporated under vacuum and the resulting residue is dissolved in DCM and extracted with water, the organic layer was dried with anhydrous sodium sulfate and evaporated under vacuum to obtain the tert-butyl (S)-2-(diethylcarbamoyl)pyrrolidine-1-carboxylate. In a solution of tert-butyl (S)-2-(diethylcarbamoyl)pyrrolidine-1-carboxylate (1.2 g, 4.65 mmol) in 5 mL DCM, 5 mL trifluoroacetic acid was added and the reaction was stirred at room temperature for 2 hours. The solvents were evaporated to obtain (S)-*N,N*-diethylpyrrolidine-2-carboxamide which was used in the next step without further purification. To a solution of 7-acetyl coumarin carboxylic acid **11** (545 mg, 2.64 mmol) in 10 mL DCM and DMF (1:1), EDC (1.13 g, 5.87 mmol) and HOBt (899 mg, 5.87 mmol) were added, and the reaction was stirred at room temperature for 10–15 minutes. To this reaction mixture, (S)-*N,N*-diethylpyrrolidine-2-carboxamide (500 mg, 2.94 mmol) and Hunig's base (2.56 mL, 14.7 mmol) was added and the reaction was heated at 50 °C overnight. Upon completion of the reaction, the solution was quenched with 3 N HCl followed by aqueous NaOH and extracted with DCM. The organic layer was separated, dried with anhydrous sodium sulfate, and evaporated under vacuum. The crude product was purified by flash column chromatography using 10% MeOH/DCM as eluent to afford the corresponding coumarin amide **3c**. Off white solid, yield (432 mg, 41% Yield). 7:5 rotamers. ^1H NMR (500 MHz, DMSO- d_6): Rotamer 1: δ 8.12 (s, 1H), 7.56 (d, $J=7.0$ Hz, 1H), 6.87–6.84 (m, 1H), 6.77 (s, 1H), 4.95–4.92 (m, 1H), 3.78–3.06 (m, 6H), 2.48–1.89 (m, 4H), 1.35 (t, $J=6.0$ Hz, 3H), 1.17 (t, $J=6.0$ Hz, 3H). ^{13}C NMR (125 MHz, DMSO- d_6): δ 171.7, 164.7, 163.0, 158.6, 156.3, 144.2, 130.4, 119.6, 113.8, 110.9, 102.0, 57.3, 48.6, 42.0, 40.8, 29.5, 24.5, 13.1, 11.7; Rotamer 2: δ 7.87 (s, 1H), 7.52 (d, $J=7.0$ Hz, 1H), 6.87–6.84 (m, 1H), 6.75 (s, 1H), 4.79–4.77 (m, 1H), 3.78–3.06 (m, 6H), 2.48–1.89 (m, 4H), 0.88 (t, $J=6.0$ Hz, 3H), 0.79 (t, $J=6.0$ Hz, 3H). ^{13}C NMR (125 MHz, DMSO- d_6): δ 171.5, 165.3, 163.2, 158.6, 156.2, 144.8, 130.4, 119.6, 113.9, 110.8, 101.9, 58.2, 48.6, 41.6, 40.8, 31.3, 22.5, 12.8, 11.7; HRMS-ESI (m/z): $[\text{M} + \text{H}]^+$: calc. for $\text{C}_{19}\text{H}_{23}\text{N}_2\text{O}_5$ 359.1602, found 359.1595.

General method for the synthesis of coumarin phenyl amides 3d and 3e: To a solution of coumarin carboxylic acid (1 g, 5.26 mmol) in 10 mL DCM, EDC (1.21 g, 6.31 mmol) and DMAP (771 mg, 6.31 mmol) was added. The reaction mixture was stirred for 10–15 minutes at room temperature and aniline (539 mg, 5.79 mmol) was added followed by triethylamine (2.2 mL, 15.78 mmol) and the reaction was heated at 50 °C overnight. The reaction was quenched with water and extracted with DCM and the organic layer was separated and dried using anhydrous sodium sulfate. The organic layer was evaporated under vacuum and the crude product was purified via recrystallization using ethyl acetate.

2-oxo-*N*-phenyl-2H-chromene-3-carboxamide (3d): Off white solid, yield (1.23 g, 88% yield). ^1H NMR (400 MHz, DMSO- d_6): δ 10.86 (s, 1H), 9.05 (s, 1H), 7.78–7.71 (m, 4H), 7.49–7.39 (m, 4H), 7.19 (t, $J=7.5$ Hz, 1H). ^{13}C NMR (100 MHz, DMSO- d_6): δ 161.8, 159.3, 154.5, 149.0, 137.7, 134.4, 130.0, 129.1, 125.5, 124.8, 120.6, 118.7, 118.7, 116.7. HRMS-ESI (m/z): $[\text{M} + \text{H}]^+$: calc. for $\text{C}_{16}\text{H}_{12}\text{NO}_3$ 266.0812, found 266.0812.

7-(diethylamino)-2-oxo-*N*-phenyl-2H-chromene-3-carboxamide (3e): Pale yellow solid, yield (830 mg, 72%). ^1H NMR (500 MHz, DMSO- d_6): δ 10.75 (s, 1H), 8.78 (s, 1H), 7.75–7.70 (m, 3H), 7.37 (t, $J=7.6$ Hz, 2H), 7.12 (t, $J=7.0$ Hz, 1H), 6.85 (d, $J=9.0$ Hz, 1H), 6.68 (s, 1H), 3.51 (q, $J=6.8$ Hz, 4H), 1.16 (t, $J=6.8$ Hz, 6H). ^{13}C NMR (125 MHz, DMSO- d_6): δ 162.7, 161.2, 157.9, 153.3, 148.7, 138.7, 132.3, 129.5, 124.3, 120.2, 110.9, 109.6, 108.4, 96.4, 44.9, 12.8. HRMS-ESI (m/z): $[\text{M} + \text{H}]^+$: calc. for $\text{C}_{20}\text{H}_{21}\text{N}_2\text{O}_3$ 337.1547, found 337.1543.

Synthesis of ethyl 7-((3-methylbut-2-en-1-yl)oxy)-2-oxo-2H-chromene-3-carboxylate (4a): To a solution of **1f** (500 mg, 2.13 mmol) in acetonitrile (10 mL), 3,3-dimethylallylbromide (0.3 mL, 2.56 mmol) and sodium carbonate (453 mg, 4.27 mmol) was added and stirred at room temperature overnight. Upon completion, the solvent was evaporated and extracted with EtOAc-water. The organic layer was dried using sodium sulfate and evaporated under vacuum to obtain the crude product, which was purified via column chromatography in EtOAc-hexanes (5%) to get ethyl 7-((3-methylbut-2-en-1-yl)oxy)-2-oxo-2H-chromene-3-carboxylate **4a** as a pale brown solid, yield (450 mg, 70% yield). ^1H NMR (500 MHz, DMSO- d_6): δ 8.52 (s, 1H), 7.51 (d, $J=9.0$ Hz, 1H), 6.92–6.90 (m, 1H), 6.61 (d, $J=2.0$ Hz, 1H), 5.51–5.47 (m, 1H), 4.63 (d, $J=7.0$ Hz, 2H), 4.42 (q, $J=7.0$ Hz, 2H), 1.84 (s, 3H), 1.80 (s, 3H), 1.43 (t, $J=7.0$ Hz, 3H). ^{13}C NMR (125 MHz, DMSO- d_6): δ 164.5, 163.5, 157.5, 157.3, 149.1, 139.8, 130.7, 118.2, 114.3, 113.9, 111.5, 101.0, 65.7, 61.7, 25.8, 18.3, 14.3. HRMS-ESI (m/z): $[\text{M} + \text{H}]^+$: calc. for $\text{C}_{17}\text{H}_{19}\text{O}_5$ 303.1227, found 303.1252.

Synthesis of 7-((3-methylbut-2-en-1-yl)oxy)-2-oxo-2H-chromene-3-carboxylic acid (4b): To a solution of **4a** (450 mg, 1.49 mmol) in 10 mL THF-water (1:1), sodium hydroxide (453 mg, 4.27 mmol) was added and the reaction was stirred at 50 °C overnight. The reaction was quenched with ice-cold 3 N HCl and the resulting solid was filtered and washed with water and hexanes. The crude product was purified via column chromatography using EtOAc-hexanes (60–80%) to obtain **4b** as a pale grey solid. (352 mg, 60% yield). ^1H NMR (400 MHz, DMSO- d_6): δ 12.96 (s, 1H), 8.72 (s, 1H), 7.82 (d, $J=8.8$ Hz, 1H), 7.04–6.98 (m, 2H), 5.46 (t, $J=6.8$ Hz, 1H), 4.68 (d, $J=6.8$ Hz, 2H), 1.75 (d, $J=10.8$ Hz, 6H). ^{13}C NMR (100 MHz, DMSO- d_6): δ 164.6, 132.0, 119.3, 114.2, 114.1, 112.0, 101.3, 65.9, 40.6, 40.4, 39.6, 39.4, 25.9, 18.5. HRMS-ESI (m/z): $[\text{M} + \text{H}]^+$: calc. for $\text{C}_{15}\text{H}_{15}\text{O}_5$ 275.0914, found 275.0946.

Synthesis of (E)-3-(3-(ethoxycarbonyl)-2-oxo-2H-chromen-6-yl)acrylic acid (4c): To a round bottom flask charged with 6-bromo coumarin carboxylic acid ethyl ester (360 mg, 1.21 mol), Pd(OAc) $_2$ (27.2 mg, 0.12 mmol), P(*p*-OCH $_3$ Ph) $_3$ (51.2 mg, 0.15 mmol), 10 mL toluene was added, and the flask was flushed with nitrogen gas, followed by the addition of tert-butyl acrylate (0.35 mL, 2.42 mmol) and triethyl-

amine (0.51 mL, 3.64 mmol). The reaction mixture was heated at 90 °C overnight and the contents were filtered, washed with ethyl acetate and the filtrate was evaporated under vacuum. The crude product was purified via column chromatography. To a solution of *tert* butyl ester derivative (300 mg, 0.87 mmol) in 10 mL toluene, silica gel (300 mg) was added, and the reaction was refluxed for 2–4 hours. The contents were filtered, washed with ethyl acetate and evaporated to obtain the pure product. Pale yellow solid, (220 mg, 63% yield). ¹H NMR (500 MHz, DMSO-*d*₆): δ 12.60 (*br s*, 1H), 8.70 (*s*, 1H), 8.23 (*d*, *J*=2.0 Hz, 1H), 8.06 (*dd*, *J*=9.0, 2.0 Hz, 1H), 7.60 (*d*, *J*=16.0 Hz, 1H), 7.47 (*d*, *J*=9.0 Hz, 1H), 6.60 (*d*, *J*=16.0 Hz, 1H), 4.31 (*q*, *J*=7.0 Hz, 2H), 1.32 (*t*, *J*=7.0 Hz, 3H). ¹³C NMR (125 MHz, DMSO-*d*₆): δ 168.1, 162.9, 156.2, 155.7, 148.8, 141.8, 134.2, 131.6, 130.3, 121.4, 118.7, 118.6, 117.3, 61.8, 14.5. HRMS-ESI (*m/z*): [M + H]⁺: calc. for C₁₅H₁₃O₆ 289.0707, found 289.0711.

Synthesis of 7-hydroxy-3-(phenylsulfonyl)-2H-chromen-2-one (5): To a solution of thiophenol (2 g, 18.15 mmol) and ethylbromoacetate (2.88 g, 17.25 mmol) in 10 mL acetonitrile, K₂CO₃ (7.53 g, 54.46 mmol) was added, and the reaction was stirred at room temperature overnight. The reaction was filtered, evaporated, and extracted with EtOAc-water and the organic layer was dried using anhydrous sodium sulfate and evaporated under vacuum to obtain ethyl 2-(phenylthio)acetate **4d**, which was used in the next step without further purification. To a solution of **4d** (1.5 g, 7.6 mmol) in 25 mL acetonitrile and water (1:1), oxone (7.0 g, 11 mmol) was added and the reaction mixture was stirred at room temperature for 2 hours. Upon completion, the reaction was poured into ice-cold water and the resulting solution was extracted with EtOAc-water to obtain ethyl 2-(phenylsulfonyl)acetate **4e**, which was used in the next step without further purification. To a solution of 2,4-dihydroxybenzaldehyde (645 mg, 4.67 mmol) in 10 mL acetonitrile, **4e** (1.25 g, 5.60 mmol) and piperidine (0.46 mL, 4.67 mmol) was added and the reaction was stirred at room temperature overnight. The reaction mixture was poured into ice-cold 3 N HCl and stirred to obtain solid, which was filtered and washed with water and hexanes. The crude product was purified via column chromatography using EtOAc-Hexanes (70%). Pale brown solid, yield (800 mg, 57%). ¹H NMR (500 MHz, DMSO-*d*₆): δ 11.33 (*br s*, 1H), 9.00 (*s*, 1H), 7.99 (*d*, *J*=8.5 Hz, 2H), (*dd*, *J*=5.0, 3.5 Hz, 1H), 7.73 (*t*, *J*=7.0 Hz, 1H), 7.64 (*t*, *J*=8.0 Hz, 1H), 6.92 (*dd*, *J*=8.5, 2.0 Hz, 1H), 6.76 (*d*, *J*=2.0 Hz, 1H). ¹³C NMR (125 MHz, DMSO-*d*₆): δ 165.5, 158.0, 155.6, 149.5, 139.7, 134.4, 133.7, 129.6, 128.7, 121.7, 115.1, 110.4, 102.6. HRMS-ESI (*m/z*): [M + H]⁺: calc. for C₁₅H₁₁O₅S 303.0322, found 303.0328.

Biology

Cell lines and culture conditions: Wild type DuCaP and LNCaP cells were obtained from ATCC and cultured in RPMI-1640 medium supplemented with 10% FBS, and penicillin-streptomycin (50 U/mL, 50 µg/mL). WPMY-1 cells were obtained from ATCC and cultured in DMEM medium supplemented with 10% FBS, and penicillin-streptomycin (50 U/mL, 50 µg/mL). AKR1C3 overexpressing LNCaP1C3 cells were generated by stable transfection of AKR1C3 plasmid as previously described.^[44] 22Rv1 human prostate cancer cell line (ATCC) was cultured in RPMI-1640 medium supplemented with 10% FBS (Sigma), and penicillin-streptomycin (50 U/mL, 50 µg/mL, Invitrogen). 22Rv1, LNCaP, and LNCaP1C3 cells tested negative for mycoplasma contamination in April 2024. Newly-established human T-cell ALL cell line, COG-LL-317h,^[45] and pre-B-cell ALL cell line, TX-LL-057h, were obtained from the Alex's Lemonade Stand Foundation/Children's Oncology Group Repository at Texas Tech University Health Sciences Center (www.CCcells.org). Both COG-LL-317h and TX-LL-057h are grown in a base medium of Iscove's Modified Dulbecco's Medium plus the following supplements (to a final concentration): 20% Fetal Bovine Serum, 4 mM L-Glutamine,

1X ITS (5 µg/mL insulin, 5 µg/mL transferrin, 5 ng/mL selenous acid) in bone marrow-level hypoxia (5% O₂).

AKR enzyme inhibition assay: (S)-(+)-1,2,3,4-tetrahydro-1-naphthol (S-tetralol) was purchased from Sigma-Aldrich (St. Louis, MO). Nicotinamide adenine dinucleotide (NAD⁺) and nicotinamide adenine dinucleotide phosphate (NADP⁺) were purchased from Roche Diagnostics (Indianapolis, IN). Homogeneous recombinant enzymes AKR1C1, AKR1C2, AKR1C3 and AKR1C4 were prepared and purified as previously described.^[46] The specific activities of the enzymes were as follows for the oxidation of S-tetralol: AKR1C2 and AKR1C3 were 1.5 and 3.5 µmol min⁻¹ mg⁻¹, respectively; and for the oxidation of androsterone AKR1C4 had a specific activity of 0.32 µM/min/mg.

Assay of enzyme activity: The dehydrogenase activities of AKR1C2, and AKR1C3 were determined by measuring the formation of NADH formation at 340 nm using Beckman DU640 spectrophotometer. A typical assay solution contained 100 mM potassium phosphate pH 7.0, 2.3 mM NAD⁺, 3.0 mM (S)-(+)-1,2,3,4-tetrahydro-1-naphthol (S-tetralol), 4% acetonitrile (v/v). The mixtures were incubated at 37 °C for 3 min followed by adding a serial dilution of AKR1C2, or AKR1C3 solution to a final volume of 1 mL to initiate the reaction. After continuously monitoring for 5 min, the increase in UV absorption using different concentrations of enzyme were recorded to calculate the initial velocity and determine enzyme specific activity.

IC₅₀ value determination: The inhibitory potency for each compound was represented by IC₅₀ value and measured as described before.^[47] The IC₅₀ value of coumarin analogues was determined by measuring their inhibition of the NADP⁺ dependent oxidation of S-tetralol catalyzed by AKR1C1, AKR1C2, and AKR1C3 in a 96-well plate format and the reaction measured fluorometrically with a (Exc/Emi, 340/460 nm) on a BIOTEK Synergy 2 Multimode plate reader. The assay mixture consisted of 100 mM phosphate buffer, pH 7.0, S-tetralol (in DMSO), inhibitor (in DMSO), 200 µM NADP⁺, and purified recombinant enzyme to give a total volume of 200 µL, and 4% DMSO. The concentration of S-tetralol used in the assays for each AKR1C isoform was equal to the K_m value for the respective enzyme so that IC₅₀ values could be directly compared assuming a competitive pattern of inhibition. The K_m value obtained for S-tetralol for AKR1C2 and AKR1C3 under the same experimental conditions were 15 µM and 165 µM, respectively. The IC₅₀ value of each compound was acquired from a single experiment with each inhibitor concentration run in quadruplicate and directly calculated by fitting the inhibition data to an equation [y=(range)/[1+(I/IC₅₀)^S]+background] using Grafit 5.0 software. In this equation, "range" is the fitted uninhibited value minus the "background", and "S" is a slope factor. "I" is the concentration of inhibitor. The equation assumes that y falls with increasing "I".

Docking: Docking experiments were performed with SeeSAR 12.1 software (BioSolveIT, Sankt Augustin, Germany). The crystal structure of AKR1C3 (PDB ID: 7C7G) and AKR1C2 (PDB ID: 4JQ4) were separately imported into the binding site tool as a PDB file. The reference ligand was removed, and the binding site defined as an amino acid residue pocket directly surrounding the template ligand. The default parameter settings of SeeSAR were used. Compounds were prepared and docked with FlexX, wherein fragments are placed into multiple places in the defined pocket and scored with a pre-scoring system.^[50]

FlexS,^[51] was used to generate compound/reference ligand superimposition to determine similarity between the test compound and the reference ligand, providing a ranked list for prioritizing compounds. Binding poses were scored by hydrogen dehydration (HYDE),^[52] and the top 20 scoring binding poses of each compound

were imported and analyzed in SeeSAR. The top scoring pose was selected based on estimated affinity, ligand efficiency, and torsion energy. Individual compound docking figures are generated from a perspective to illustrate binding interactions in the most accessible way in a 2D figure, and therefore do not represent a fixed orientation or perspective.

Growth Inhibition Assay: 1.5×10^4 DuCaP cells in RPMI media in 100 μL 5% charcoal dextran stripped FBS were plated per well in a 96-plate format. After 24 h 100 μL media containing 1.0 nM 4-androstene-3,17-dione, inhibitor were added to the wells where the DMSO concentration was 1%. Cell number was counted on a Biotek Cytation plate reader daily over 10 days exposure.

Clonogenic survival assay: 22Rv1 cells, cultured in 20% O_2 and 5% CO_2 at 37 $^\circ\text{C}$, were seeded into T25 flasks at a density of 3×10^5 cells/flask to ensure logarithmic growth during treatment. The following day cells were treated with 10 μM compound or an equal volume of DMSO and incubated under normal cell culture conditions for 48 hours. Cells were then irradiated with 2 Gy of X-rays or sham irradiated for the 0 Gy conditions. Immediately following radiation, the cells were detached and serially diluted to 200 (0 Gy) or 800 (2 Gy) cells/mL and seeded into 6 well plates. The cultures were allowed to grow undisturbed for 14 days. Colonies were fixed to the plates with 70% ethanol then stained with 0.5% crystal violet in 25% methanol. Using a dissecting microscope, colonies containing 50 or more cells were counted clonogenically viable, and the surviving fraction calculated based on the plating efficiency of the sham control. All conditions were performed $n=3$ times and the mean surviving fraction is reported.

Liquid chromatography and mass spectrometry (LC–MS/MS) conditions: A Shimadzu 8060 NX mass and Nexera Series liquid chromatograph (Shimadzu Scientific Instruments, Columbia, MD). The MS/MS system was operated at unit resolution in the multiple reaction monitoring (MRM) in positive ESI mode, using precursor ion > product ion combinations of 260.20 > 132.10 m/z for 3a. The analytical column was an Acquity UPLC[®] BEH C18, 2.1 \times 100 mm, 1.7 μm column (Waters, Inc. Milford MA) was used to separate the 3a analytes and the internal standard (IS). The mobile phase consisted of water containing 0.1% formic acid (Phase A) and methanol (Phase B) at a flow rate of 0.25 mL/min with an operating temperature of room temperature. The total run time was set to last 7.5 min with a gradient elution system.

In-vitro metabolic stability in HLM/MLM: Metabolic stability was assessed using HLM and MLM (XenoTech, LLC, Lenexa, KS). All incubations with 3a (2 μM) were performed in triplicate, as previously described.^[53] The reaction was started by adding 2 μL of 3a at a final concentration of 2 μM . Serial samples (50 μL) were collected at selected time intervals and quenched with 300 μL of methanol spiked with 10 μL of IS (0.5 $\mu\text{g}/\text{mL}$). All samples were vortexed and centrifuged at 13,000 g for 15 min, and the supernatant was collected and transferred to an autosampler vial and injected (2 μL) onto the LC–MS/MS system. Testosterone was used as a positive control to ensure incubation conditions were appropriate to conduct metabolism studies. Microsomal stability was expressed as the percentage of drug remaining at each sample time.

Mouse plasma stability studies of 3a: Plasma stability of 3a was determined in mouse plasma at concentrations of 2 μM . Incubation with mouse plasma was performed in triplicate, at 37 $^\circ\text{C}$ on a shaking water bath for 4 hours. Samples (50 μL) were collected at 0, 30, 60, 120 and 240 minutes. Immediately after sample collection, five volumes of methanol containing IS was added and samples were prepared for analysis. Stability was determined as a percentage of parent compound detected at each time point relative to

the concentration at 0 minutes. Plasma stability was expressed as the percentage of drug remaining at each time.

DIMSCAN assay: Activity of drugs against leukemia cell lines was evaluated by the DIMSCAN assay. Test compounds were pretreated for 24 hours to a maximum concentration of 80 μM before addition of chemotherapeutic. Maximum dose of chemotherapeutic was ABT-737 5 μM , daunorubicin 265 μM , and dexamethasone 500 nM. Cells were incubated with single compound or combination for 72 hours before DIMSCAN assay, which was performed as previously described.^[43]

Acknowledgements

Research reported in this publication was supported in part by the National Cancer Institute of the National Institutes of Health under Award Number R01 CA226436 (P.C.T) and by the National Institute of Environmental Health Sciences P30 ES01308 (T.M.P) Content is solely the responsibility of the authors and does not necessarily represent the official views of the National Institutes of Health.

Conflict of Interests

T.M.P. is a member of the Expert Panel for Research Institute for Fragrance Materials, is founder of Penzymes and a consultant for Propella and Sage Therapeutics.

Data Availability Statement

The data that support the findings of this study are available in the supplementary material of this article.

Keywords: AKR1C3 Inhibitor · AKR1C2 Inhibitor · Prostate Cancer · Leukemia · Drug Resistance

- [1] T. L. Rizner, T. M. Penning, *Pharmacol. Res.* **2020**, *152*, 104446.
- [2] T. M. Penning, P. Wangtrakuldee, R. J. Auchus, *Endocr Rev* **2019**, *40*, 447–475.
- [3] T. M. Penning, S. Jonnalagadda, P. C. Trippier, T. L. Rizner, *Pharmacol. Rev.* **2021**, *73*, 1150–1171.
- [4] P. Velica, N. J. Davies, P. P. Rocha, H. Schrewe, J. P. Ride, C. M. Bunce, *Mol. Cancer* **2009**, *8*, 121.
- [5] K. Verma, T. Zang, T. M. Penning, P. C. Trippier, *J. Med. Chem.* **2019**, *62*, 3590–3616.
- [6] K. Verma, N. Gupta, T. Zang, P. Wangtrakuldee, S. K. Srivastava, T. M. Penning, P. C. Trippier, *Mol. Cancer Ther.* **2018**, *17*, 1833–1845.
- [7] K. Verma, T. Zang, N. Gupta, T. M. Penning, P. C. Trippier, *ACS Med. Chem. Lett.* **2016**, *7*, 774–779.
- [8] T. Zang, K. Verma, M. Chen, Y. Jin, P. C. Trippier, T. M. Penning, *Chem. Biol. Interact.* **2015**, *234*, 339–348.
- [9] D. Reddi, B. W. Seaton, D. Woolston, L. Aicher, L. D. Monroe, Z. J. Mao, J. C. Harrell, J. P. Radich, A. Advani, N. Papadantonakis, C. C. S. Yeung, *Sci. Rep.* **2022**, *12*, 5809.
- [10] A. C. Pippione, Z. Kilic-Kurt, S. Kovachka, S. Sainas, B. Rolando, E. Denasio, K. Pors, S. Adinolfi, D. Zonari, R. Bagnati, M. L. Lolli, F. Spyraakis, S. Oliaro-Bosso, D. Boschi, *Eur. J. Med. Chem.* **2022**, *237*, 114366.
- [11] Y. Liu, S. He, Y. Chen, Y. Liu, F. Feng, W. Liu, Q. Guo, L. Zhao, H. Sun, *J. Med. Chem.* **2020**, *63*, 11305–11329.

- [12] S. Endo, H. Oguri, J. Segawa, M. Kawai, D. Hu, S. Xia, T. Okada, K. Irie, S. Fujii, H. Gouda, K. Iguchi, T. Matsukawa, N. Fujimoto, T. Nakayama, N. Toyooka, T. Matsunaga, A. Ikari, *J. Med. Chem.* **2020**, *63*, 10396–10411.
- [13] M. L. Lolli, I. M. Carnovale, A. C. Pippione, W. Y. Wahlgren, D. Bonanni, E. Marini, D. Zonari, M. Gallicchio, V. Boscaro, P. Goyal, R. Friemann, B. Rolando, R. Bagnati, S. Adinolfi, S. Oliaro-Bosso, D. Boschi, *ACS Med. Chem. Lett.* **2019**, *10*, 437–443.
- [14] A. C. Pippione, I. M. Carnovale, D. Bonanni, M. Sini, P. Goyal, E. Marini, K. Pors, S. Adinolfi, D. Zonari, C. Festuccia, W. Y. Wahlgren, R. Friemann, R. Bagnati, D. Boschi, S. Oliaro-Bosso, M. L. Lolli, *Eur. J. Med. Chem.* **2018**, *150*, 930–945.
- [15] A. Adeniji, M. J. Uddin, T. Zang, D. Tamae, P. Wangtrakuldee, L. J. Marnett, T. M. Penning, *J. Med. Chem.* **2016**, *59*, 7431–7444.
- [16] Y. D. Yin, M. Fu, D. G. Brooke, D. M. Heinrich, W. A. Denny, S. M. Jamieson, *Front. Oncol.* **2014**, *4*, 159.
- [17] K. Maddeboina, S. K. Jonnalagadda, A. Morsy, L. Duan, Y. S. Chhonker, D. J. Murry, T. M. Penning, P. C. Trippier, *J. Med. Chem.* **2023**, *66*, 9894–9915.
- [18] F. Khanim, N. Davies, P. Velica, R. Hayden, J. Ride, C. Pararasa, M. G. Chong, U. Gunther, N. Veerapen, P. Winn, R. Farmer, E. Trivier, L. Rigoreau, M. Drayson, C. Bunce, *Br. J. Cancer* **2014**, *110*, 1506–1516.
- [19] R. Bortolozzi, S. Bresolin, E. Rampazzo, M. Paganin, F. Maule, E. Mariotto, D. Boso, S. Minuzzo, V. Agnusdei, G. Viola, G. Te Kronnie, G. Cazzaniga, G. Basso, L. Persano, *Br. J. Cancer* **2018**, *118*, 985–994.
- [20] W. Xiong, J. Zhao, H. Yu, X. Li, S. Sun, Y. Li, Q. Xia, C. Zhang, Q. He, X. Gao, L. Zhang, D. Zhou, *PLoS One* **2014**, *9*, e111911.
- [21] L. Xie, J. Yu, W. Guo, L. Wei, Y. Liu, X. Wang, X. Song, *Cancer Gene Ther.* **2013**, *20*, 260–266.
- [22] S. Q. Sun, X. Gu, X. S. Gao, Y. Li, H. Yu, W. Xiong, H. Yu, W. Wang, Y. Li, Y. Teng, D. Zhou, *Oncotarget* **2016**, *7*, 48050–48058.
- [23] X. Li, X. Hong, X. Gao, X. Gu, W. Xiong, J. Zhao, H. Yu, M. Cui, M. Xie, Y. Bai, S. Sun, *Cancer Manag. Res.* **2018**, *10*, 3149–3158.
- [24] O. M. Tsvileva, O. V. Koftin, N. V. Evseeva, *Antibiotics (Basel)* **2022**, *11*, 1156.
- [25] N. Bhattarai, A. A. Kumbhar, Y. R. Pokharel, P. N. Yadav, *Mini Rev. Med. Chem.* **2021**, *21*, 2996–3029.
- [26] S. Gurrapu, S. K. Jonnalagadda, M. A. Alam, C. T. Ronayne, G. L. Nelson, L. N. Solano, E. A. Lueth, L. R. Drewes, V. R. Mereddy, *Bioorg. Med. Chem. Lett.* **2016**, *26*, 3282–3286.
- [27] S. K. Jonnalagadda, B. I. Huwaimel, S. Jonnalagadda, J. C. Garrison, P. C. Trippier, *J. Org. Chem.* **2022**, *87*, 4476–4482.
- [28] M. Sinreih, R. Jojart, Z. Kele, T. Budefeld, G. Paragi, E. Mernyak, T. L. Rizner, *J. Enzyme Inhib. Med. Chem.* **2021**, *36*, 1500–1508.
- [29] K. M. Chang, H. H. Chen, T. C. Wang, I. L. Chen, Y. T. Chen, S. C. Yang, Y. L. Chen, H. H. Chang, C. H. Huang, J. Y. Chang, C. Shih, C. C. Kuo, C. C. Tzeng, *Eur. J. Med. Chem.* **2015**, *106*, 60–74.
- [30] D. Li, E. M. Ellis, *Neurotoxicology* **2012**, *33*, 1368–1374.
- [31] S. Endo, T. Matsunaga, K. Kuwata, H. T. Zhao, O. El-Kabbani, Y. Kitade, A. Hara, *Bioorg. Med. Chem.* **2010**, *18*, 2485–2490.
- [32] S. Endo, S. Xia, M. Suyama, Y. Morikawa, H. Oguri, D. Hu, Y. Ao, S. Takahara, Y. Horino, Y. Hayakawa, Y. Watanabe, H. Gouda, A. Hara, K. Kuwata, N. Toyooka, T. Matsunaga, A. Ikari, *J. Med. Chem.* **2017**, *60*, 8441–8455.
- [33] T. Matsunaga, Y. Yamane, K. Iida, S. Endo, Y. Banno, O. El-Kabbani, A. Hara, *Anticancer Drugs* **2011**, *22*, 402–408.
- [34] J. Park, S. B. Paudel, C. H. Jin, G. Lee, H. I. Choi, G. H. Ryoo, Y. S. Kil, J. W. Nam, C. H. Jung, B. R. Kim, M. K. Na, A. R. Han, *Molecules* **2022**, *27*, 7391.
- [35] M. Ashraf-Uz-Zaman, S. Shahi, R. Akwii, M. S. Sajib, M. J. Farshbaf, R. R. Kallem, W. Putnam, W. Wang, R. Zhang, K. Alvina, P. C. Trippier, C. M. Mikelis, N. A. German, *Eur. J. Med. Chem.* **2021**, *209*, 112866.
- [36] A. R. Hamid, M. J. Pfeiffer, G. W. Verhaegh, E. Schaafsma, A. Brandt, F. C. Sweep, J. P. Sedelaar, J. A. Schalken, *Mol. Med.* **2013**, *18*, 1449–1455.
- [37] H. Neuwirt, J. Bouchal, G. Kharashvili, C. Ploner, K. Johrer, F. Pitterl, A. Weber, H. Klocker, I. E. Eder, *Cell Commun. Signal* **2020**, *18*, 11.
- [38] A. J. Detlefsen, C. A. Mesaros, L. Duan, T. M. Penning, *Cancer Res. Commun.* **2023**, *3*, 1888–1898.
- [39] A. J. Liedtke, A. O. Adeniji, M. Chen, M. C. Byrns, Y. Jin, D. W. Christianson, L. J. Marnett, T. M. Penning, *J. Med. Chem.* **2013**, *56*, 2429–2446.
- [40] N. J. Davies, R. E. Hayden, P. J. Simpson, J. Birtwistle, K. Mayer, J. P. Ride, C. M. Bunce, *Cancer Res.* **2009**, *69*, 4769–4775.
- [41] N. McDermott, A. Meunier, B. Mooney, G. Nortey, C. Hernandez, S. Hurley, N. Lynam-Lennon, S. H. Barsoom, K. J. Bowman, B. Marples, G. D. Jones, L. Marignol, *Sci. Rep.* **2016**, *6*, 34796.
- [42] N. Keshelava, T. Frgala, J. Krejsa, O. Kalous, C. P. Reynolds, *Methods Mol. Med.* **2005**, *110*, 139–153.
- [43] M. H. Kang, M. A. Smith, C. L. Morton, N. Keshelava, P. J. Houghton, C. P. Reynolds, *Pediatr. Blood Cancer* **2011**, *56*, 239–249.
- [44] M. C. Byrns, R. Mindnich, L. Duan, T. M. Penning, *J. Steroid. Biochem. Mol. Biol.* **2012**, *130*, 7–15.
- [45] M. A. Sheard, M. V. Ghent, D. J. Cabral, J. C. Lee, V. Khankaldyyan, L. Ji, S. Q. Wu, M. H. Kang, R. Sposito, S. Asgharzadeh, C. P. Reynolds, *Exp. Cell Res.* **2015**, *334*, 78–89.
- [46] T. M. Penning, M. E. Burczynski, J. M. Jez, C.-F. Hung, H.-K. Lin, H. Ma, M. Moore, N. Palackal, K. Ratnam, *Biochem. J.* **2000**, *351*, 67.
- [47] A. O. Adeniji, B. M. Twenter, M. C. Byrns, Y. Jin, M. Chen, J. D. Winkler, T. M. Penning, *J. Med. Chem.* **2012**, *55*, 2311–2323.
- [48] A. O. Adeniji, B. M. Twenter, M. C. Byrns, Y. Jin, J. D. Winkler, T. M. Penning, *Biorg. Med. Chem. Lett.* **2011**, *21*, 1464–1468.
- [49] A. J. Liedtke, A. O. Adeniji, M. Chen, M. C. Byrns, Y. Jin, D. W. Christianson, L. J. Marnett, T. M. Penning, *J. Med. Chem.* **2013**, *56*, 2429–2446.
- [50] M. Rarey, B. Kramer, T. Lengauer, G. Klebe, *J. Mol. Biol.* **1996**, *261*, 470–489.
- [51] C. Lemmen, T. Lengauer, G. Klebe, *J. Med. Chem.* **1998**, *41*, 4502–4520.
- [52] N. Schneider, G. Lange, S. Hindle, R. Klein, M. Rarey, *J. Comput. Aided Mol. Des.* **2013**, *27*, 15–29.
- [53] W. N. Aldhafiri, Y. S. Chhonker, Y. Zhang, D. W. Coutler, T. R. McGuire, R. Li, D. J. Murry, *Molecules* **2020**, *25*, 5898.
- [54] V. Bala, Y. S. Chhonker, R. L. Sleightholm, A. J. Crawford, M. A. Hollingsworth, D. J. Murry, *Biomed. Chromatogr.* **2020**, *34*, e4859.

Manuscript received: January 25, 2024

Revised manuscript received: June 28, 2024

Accepted manuscript online: July 8, 2024

Version of record online: September 16, 2024